ANALYSIS OF STRUCTURAL RESPONSE UNDER BLAST LOADING USING SAP 2000® AND AUTODYN®

Project Report submitted in partial fulfillment of the requirement for the degree of

Master of Technology

In

Structural Engineering

Under the Supervision of

Mr. Anil Dhiman

By

Ashish Kumar Tiwari

(132662)

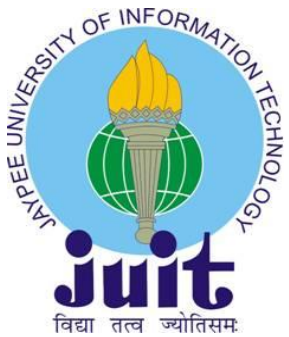

Department of Civil Engineering

Jaypee University of Information and Technology
Waknaghat, Solan – 173234, Himachal Pradesh 2015

CERTIFICATE

This is to certify that the work which is being presented in the project title **"ANALYSIS OF STRUCTURAL RESPONSE UNDER BLAST LOADING USING SAP 2000 AND AUTODYN"** in partial fulfillment of the requirements for the award of the degree of Master of technology and submitted in Civil Engineering Department, Jaypee University of Information Technology, Waknaghat is an authentic record of work carried out by **Ashish Kumar Tiwari** during a period from August 2014 to May 2015 under the supervision of **Mr. Anil Dhiman** Assistant Professor, Civil Engineering Department, Jaypee University of Information Technology, Waknaghat.

The above statement made is correct to the best of my knowledge.

Date: - ……

Prof. Dr. Ashok Kumar Gupta	Mr. Anil Dhiman	……
Professor & Head of Department	Assistant Professor	External Examiner
Civil Engineering Department	Civil Engineering Department	
JUIT Waknaghat	JUIT Waknaghat	

DECLARATION

I hereby declare that the research work presented in this Project entitled "*Analysis of Structural Response under Blast Loading Using SAP 2000 and Autodyn"* submitted for the award of the degree of Master of technology in the Department of Civil Engineering, Jaypee University of Information and Technology Wakhnaghat, is original and my own account of research. This research work is independent and its main content work has not previously been submitted for degree at any university in India or Abroad.

(Ashish Kumar Tiwari)

ACKNOWLEDGEMENT

I wish to express my sincere gratitude to **Mr. Anil Dhiman,** for his excellent guidance and perennial encouragement and support during the course of my work in the last one year. I truly appreciate and value his profound knowledge, esteemed supervision and encouragement from the beginning to the end of this thesis.

My special thanks are due to **Prof. Ashok Gupta,** Head of the Civil Engineering Department, for all the facilities provided to successfully complete this work.

I am also very thankful to all the faculty members of the department, especially Structural Engineering specialization for their constant encouragement during the project.

I also take the opportunity to thank all my friends who have directly or indirectly helped me in my project work and in the completion of this report.

Last but not the least I would like to thank my parents, who taught me the value of hard work by their own example. I would like to share this bite of happiness with my mother and father. They rendered me enormous support during the whole tenure of my stay at JUIT, Waknaghat

.

.

Date: **Ashish Kumar Tiwari**

ABSTRACT

In recent years, explosive devices are the weapon of choices for the majority of terrorist attack that not only affects the life of human being but also the structure resistance and physical integrity. Bomb explosion near the building can cause such amount of pressure and produces a large amount of heat resulting a high strain loading on building and its elements. Such a high strain loading can cause catastrophic damage on building's external and internal structural frame, collapsing of walls, blowing out large expense of windows and shutting down of critical life safety systems.

Due to such impact of this large dynamic loading, efforts have been made during the past few decades to develop methods of structural analysis and design of blast resistance structure. Since blast resistant design is the important topic of study and therefore requires the careful understanding about the blast phenomena and its effect and impact on various structural elements.

The response of steel frame building subjected to blast loading was examined by calculating blast load manually using a procedure and applying on joints. Response of steel column subjected to amount of pressure exerted by different charge weights and at different standoff distance and progressive energy collapse of steel column is examined using Ansys Explicit dynamic and Ansys Autodyn. Concrete wall subjected to blast loading is modeled in Finite Element package Ansys and then analyzed in Autodyn with and without steel plate to study the impact of blast loading.

Index

LIST OF FIGURES

LIST OF TABLES

CHAPTER 1
INTRODUCTION

1 INTRODUCTION

In the past few decades terrorist attacks and threats are the growing problem all over the world that not only affects the life of human being but also the structural resistance and its physical integrity. Also considerable emphasis has been given to problems of blast and earthquake. The earthquake problem is rather old, but most of the study and knowledge on this subject has been accumulated during the past sixty years. The blast problem is rather new; information about the development in this field is made available mostly through publication of the Army Corps of Engineers, Department of Defence, public institutes and other governmental office.

Due to different accidental or intentional events, the behaviour of structural components subjected to blast loading has been the subject of considerable research effort in recent years. Conventional structures, particularly that above grade, normally are not designed to resist blast loads; and because the magnitudes of design loads are significantly lower than those produced by most explosions, conventional structures are susceptible to damage from explosions. With this in mind, developers, architects and engineers increasingly are seeking solutions for potential blast situations, to protect building occupants and the structures

Disasters such as the terrorist bombings of the U.S. embassies in Nairobi, Kenya and Dares Salaam, Tanzania in 1998, the Khobar Towers military barracks in Dhahran, Saudi Arabia in 1996, the Murrah Federal Building in Oklahoma City in 1995, and the World Trade Centre in New York in 1993 have demonstrated the need for a thorough examination of the behaviour of columns subjected to blast loads (Kirk, et al., 2005). To provide adequate protection against explosions, the design and construction of public buildings are receiving renewed attention of structural engineers. Difficulties that arise with the complexity of the problem, which involves time dependent finite deformations, high strain rates, and non-linear inelastic material behaviour, have motivated various assumptions and approximations to simplify the models. These models span the full range of sophistication from single degree of freedom systems to general purpose finite element programs such as ABAQUS, ANSYS, and ADINA etc.

1.2 CHEMISTRY OF EXPLOSIVES

Modelling and Analysis of explosive detonations requires a good understanding of chemistry because the chemical composition of an explosive source governs its physical properties like detonation velocity. Explosive detonations are products of complex physical and chemical processes within and in the immediate vicinity of the explosive and are accompanied by a near-instantaneous release of a huge amount of energy in the form of heat, light and sound. The chemical reactions involved in a detonation are thus oxidation and exothermic reactions because the reactants are oxidized to give a mixture of hot gaseous products.

1.2.1 OXIDATION

There are two major types of oxidation reactions involved in a detonation.

a) In the first type, there are two reactants, a fuel and an oxidizer, that react to form the products of the explosion.
b) The second type of reaction, involves a single reactant where the fuel and the oxidizer are contained in the same molecule, which decomposes during the reaction and is transformed into oxidized products. It is more common in explosives.

The majority of the explosives consist of single molecules made up of Carbon (C), Hydrogen (H), Nitrogen (N) and Oxygen (O). These are called CHNO explosives and can be represented by the general formula $C_cH_hN_nO_o$, where *c*, *h*, *n*, *o* are the number of carbon, hydrogen, nitrogen and oxygen atoms, respectively, contained in one molecule of the explosive. During the decomposition2 reaction, the reactant molecule breaks down into its individual component atoms as follows

$$C_cH_hN_nO_o, \quad \rightarrow \quad cC + h\,H + nN + oO$$

These individual atoms then recombine to form the final products of the reaction. The order of reaction is

$$2N \rightarrow N2$$
$$2H + O \rightarrow H2O$$
$$C + O \rightarrow CO$$
$$CO + O \rightarrow CO2$$

If oxygen remains after the formation of carbon dioxide, then the explosive is called over-oxidized. Any oxygen left after the formation of CO_2 forms O_2. However most explosives, with the exception of nitro-glycerine and ammonium nitrate, do not have sufficient oxygen to convert all of the carbon to CO_2 and these are called under-oxidized explosives. For such explosives, the products of the reaction extract oxygen from the surrounding air as they expand freely. While doing so, these products mix with oxygen and may burn to form CO_2. These secondary reactions are part of a process known as afterburning.

The relative amount of oxygen in an explosive is therefore an important factor in determining the nature and reactivity of the detonation products; it is quantitatively expressed as oxygen balance. The heat generated by an oxygen-deficient explosive (such as trinitrotoluene (TNT)) is less than that generated by an explosive that oxidizes completely.

CHAPTER 2
LITERATURE REVIEW AND OBJECTIVES

2.1 GENERAL

The study and analysis of the blast loading on the structure started in 1960's. US Department of the Army, released a technical manual titled "structures to resist the effects of accidental explosions" in 1959. The revised edition of the manual TM 5-1300 (1990) most widely used by military and civilian organization for designing structures to prevent the propagation of explosion and to provide protection for personnel and valuable equipments.

Following methods are available for prediction of blast effects on buildings structures i.e.

- Empirical (or analytical) methods
- Semi-empirical methods
- Numerical methods

Empirical methods are essentially correlations with experimental data. Most of these approaches are limited by the extent of the underlying experimental database. The accuracy of all empirical equations diminishes as the explosive event becomes increasingly near field.

Semi-empirical methods, which are based on simplified models of physical phenomena. The attempt is to model the underlying important physical processes in a simplified way. These methods are dependent on extensive data and case study. The predictive accuracy is generally better than that provided by the empirical methods.

Numerical (or first-principle) methods are based on mathematical equations that describe the basic laws of physics governing a problem. These principles include conservation of momentum, energy, and mass. In addition, the physical behaviour of materials is described by constitutive relationships. These models are commonly termed computational fluid dynamics (CFD) models

The key elements are the loads produced from explosive sources, how they interact with structures and the way structures respond to them. Explosive sources include gas, high explosives, nuclear and dust materials. The basic features of the explosion and blast wave phenomena are presented along with a discussion of TNT (trinitrotoluene) equivalency and

blast scaling laws. The characteristics of incident overpressure loading due to atomic weapons, conventional high explosives and unconfined vapours cloud explosions are addressed and followed by a description of the other blast loading components associated with air flow and reflection process. Fertice G. has extensive study of the structures and computation of blast loading on aboveground structures.

A. Khadid et al. (2006) studied the fully fixed stiffened plates under the effect of blast loads to determine the dynamic response of the plates with different stiffener configurations and considered the effect of mesh density, time duration and strain rate sensitivity. He used the finite element method and the central difference method for the time integration of the nonlinear equations of motion to obtain numerical solutions.

A.K. Pandey et al. (2007) studied the effects of an external explosion on the outer reinforced concrete shell of a typical nuclear containment structure. The analysis has been made using appropriate non-linear material models till the ultimate stages. An analytical procedure for nonlinear analysis by adopting the above model has been implemented into a finite element code DYNAIB.

Alexander M. Remennikov (2003) studied the methods for predicting bomb blast effects on buildings. When a single building is subjected to blast loading produced by the detonation of high explosive device. Simplified analytical techniques used for obtaining conservative estimates of the blast effects on buildings. Numerical techniques including Lagrangian, Eulerian, Euler- FCT, ALE, and finite element modelling used for accurate prediction of blast loads on commercial and public buildings.

J. M. Dewey (1971) studied the properties of the blast waves obtained from the particle trajectories. First time he introduced the effect of spherical and hemispherical TNT (trinitrotoluene) in blast waves and determined the density throughout the flow by application of the Lagrangian conservation of mass equation which used for calculating the pressure by assuming the adiabatic flow for each air element between the shock fronts. The temperature and the sound speed found from the pressure and density, assuming the perfect gas equation of states.

Kirk A. Marchand et al. (2005) reviewed the contents of American Institute of Steel Construction, Inc. for facts for steel buildings give a general science of blast effects with the help of numbers of case studies of the building which are damaged due to the blast loading i.e. Murrah Building, Oklahoma City, Khobar Towers, Dhahran, Saudi Arabia and others.

Also studied the dynamic response of a steel structure to the blast loading and shows the behaviour of ductile steel column and steel connections for the blast loads.

M. V. Dharaneepathy et al. (1995) studied the effects of the stand-off distance on tall shells of different heights, carried out with a view to study the effect of distance (ground-zero distance) of charge on the blast response. An important task in blast-resistant design is to make a realistic prediction of the blast pressures. The distance of explosion from the structure is an important datum, governing the magnitude and duration of the blast loads. The distance, known as 'critical ground-zero distance', at which the blast response is a maximum. This critical distance should be used as design distance, instead of any other arbitrary distance.

Ronald L. Shope (2006) studied the response of wide flange steel columns subjected to constant axial load and lateral blast load. The finite element program ABAQUS was used to model with different slenderness ratio and boundary conditions. Non-uniform blast loads were considered. Changes in displacement time histories and plastic hinge formations resulting from varying the axial load were examined.

T. Borvik et al. (2009) studied the response of a steel container as closed structure under the blast loads. He used the mesh less methods based on the Lagrangian formulations to reduce mesh distortions and numerical advection errors to describe the propagation of blast load. All parts are modelled by shell element type in LS-DYNA. A methodology has been proposed for the creation of inflow properties in uncoupled and fully coupled Eulerian–Lagrangian LS-DYNA simulations of blast loaded structures.

TM 5-1300 (UFC 3-340-02, 1990) is a manual titled "structures to resist the effects of accidental explosions" which provides guidance to designers, the step-to-step analysis and design procedure, including the information on such items (1) blast, fragment and shock loading. (2) principle on dynamic analysis. (3) reinforced and structural steel design and (4) a number of special design considerations.

T. Ngo, et al. (2007) for their study on "Blast loading and Blast Effects on Structures" gives an overview on the analysis and design of structures subjected to blast loads phenomenon for understanding the blast loads and dynamic response of various structural elements. This study helps for the design consideration against extreme events such as bomb blast, high velocity impacts.

2.2 OBJECTIVES AND SCOPE OF THE PRESENT WORK

2.2.1 OBJECTIVES OF THE STUDY

Following are the objectives of the present work.

- To analyse a steel structure against the abnormal loading conditions requiring detailed understanding of blast phenomenon.
- To study the dynamic response of various structural elements like column, wall in FE program ANSYS Autodyn® by modelling blast with JWL (Jones-Wilkins-Lee) equation of state.
- To study analytically the structural behaviour of steel column and concrete wall subjected to blast loading.

2.2.2 SCOPE OF THE STUDY

In order to achieve the above-mentioned objectives the following tasks have been carried out.

- All the computations for dynamic loading on a steel structure to evaluate the blast pressure, using Kinney and Graham's approach.
- Computation of the blast loads on the structural joints from peak reflected pressure.
- Modelling of a steel column and concrete wall of different shapes in ANSYS Autodyn®.
- Computation of response parameters of the steel column and concrete wall under the blast loading.

CHAPTER 3
BACKGROUND

3.1 EXPLOSION AND BLAST PHENOMENON

In general, an explosion is the result of a very rapid release of large amounts of energy within a limited space. Explosions can be categorized on the basis of their nature as physical, nuclear and chemical events.

In physical explosion: - Energy may be released from the catastrophic failure of a cylinder of a compressed gas, volcanic eruption or even mixing of two liquid at different temperature.

In nuclear explosion: - Energy is released from the formation of different atomic nuclei by the redistribution of the protons and neutrons within the inner acting nuclei.

In chemical explosion: - The rapid oxidation of the fuel elements (carbon and hydrogen atoms) is the main source of energy.

The type of burst mainly classified as

a. Air burst
b. High altitude burst
c. Under water burst
d. Underground burst
e. Surface burst

The discussion in this section is limited to air burst or surface burst. This information is then used to determine the dynamic loads on surface structures that are subjected to such blast pressures and to design them accordingly. It should be pointed out that surface structure cannot be protected from a direct hit by a nuclear bomb; it can however, be designed to resist the blast pressures when it is located at some distance from the point of burst.

The destructive action of nuclear weapon is much more severe than that of a conventional weapon and is due to blast or shock. In a typical air burst at an altitude below 100,000 ft. an approximate distribution of energy would consist of 50% blast and shock, 35% thermal radiation, 10% residual nuclear radiation and 5% initial nuclear radiation (J.M. Dewey, 1971).

The sudden release of energy initiates a pressure wave in the surrounding medium, known as a shock wave as shown in Fig. 3.1 (a). When an explosion takes place, the expansion of the hot gases produces a pressure wave in the surrounding air. As this wave moves away from the centre of explosion, the inner part moves through the region that was previously compressed and is now heated by the leading part of the wave. As the pressure waves moves with the velocity of sound, the temperature is about 3000-4000 degree Celsius and the pressure is nearly 300 kilo bar of the air causing this velocity to increase. The inner part of the wave starts to move faster and gradually overtakes the leading part of the waves. After a short period of time the pressure wave front becomes abrupt, thus forming a shock front somewhat similar to Fig.3.1 (b). The maximum overpressure occurs at the shock front and is called the peak overpressure. Behind the shock front, the overpressure drops very rapidly to about one-half the peak overpressure and remains almost uniform in the central region of the explosion.

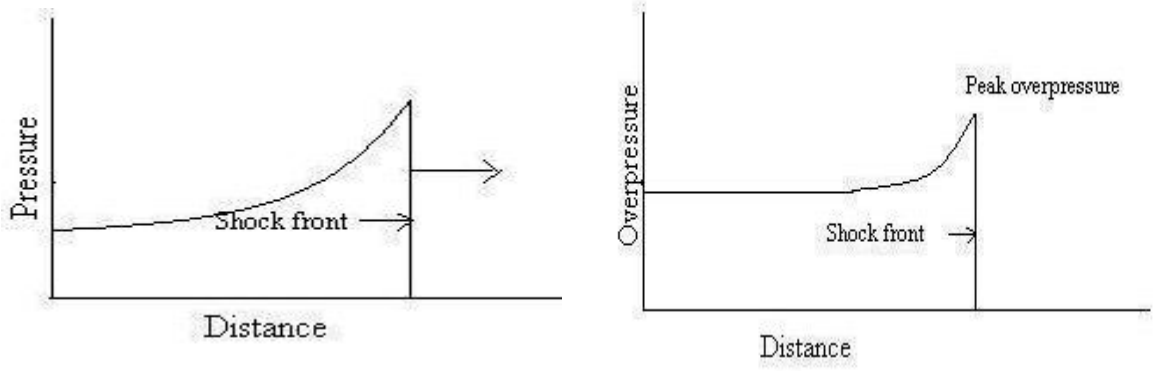

Fig.3.1 (a) Variation of pressure with distance (b) Formation of shock front in a shock wave

As the expansion proceeds, the overpressure in the shock front decreases steadily; the pressure behind the front does not remain constant, but instead, fall off in a regular manner. After a short time, at a certain distance from the centre of explosion, the pressure behind the shock front becomes smaller than that of the surrounding atmosphere and so called negative-phase or suction.

The front of the blast waves weakens as it progresses outward, and its velocity drops towards the velocity of the sound in the undisturbed atmosphere. This sequence of events is shown in the overpressure at time t1, t2…..t6 are indicated. In the curves marked t1 tot5, the pressure in the blast has not fallen below that of the atmosphere. In the curve t6 at some distance behind the shock front, the overpressure becomes negative. This is better illustrated in Fig.3.2 (a).

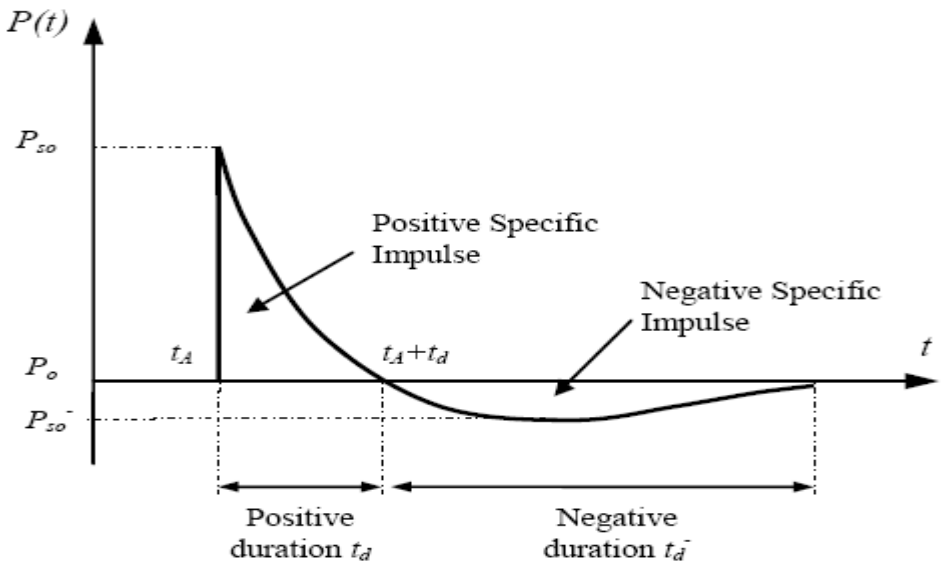

Fig.3.2 (a) The variation of overpressure with distance at a given time from centre of explosion.

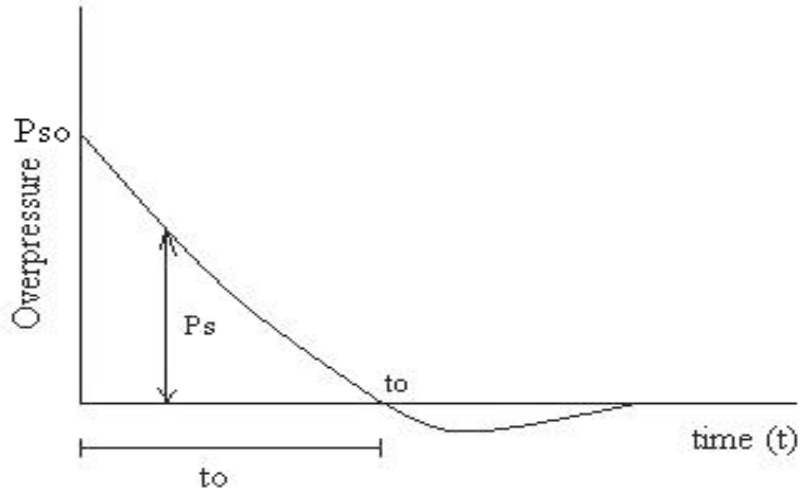

Fig.3.2 (b) Variation of overpressure with distance at a time from the explosion

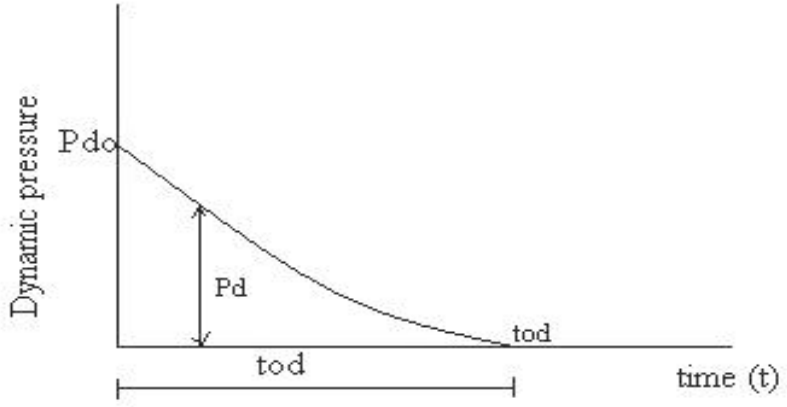

Fig.3.2(c) Variation of dynamic pressure with distance at a time from the explosion

The time variation of the same blast wave at a given distance from the explosion is shown in Fig 3.2(b); to indicate the time duration of the positive phase and also the time at the end of the positive phase. Another quantity of the equivalent importance is the force that is developed from the strong winds accompanying the blast wave known as the dynamic pressure; this is proportional to the square of the wind velocity and the density of the air behind the shock front.

Its variation at a given distance from the explosion is shown in Fig.3.2(c).

Mathematically the dynamic pressure Pd is expressed as.

$$Pd = \frac{1}{2}\rho u^2$$

where u is the velocity of the air particle and ρ is the air density

The peak dynamic pressure decreases with increasing distance from the centre of explosion, but the rate of decrease is different from that of the peak overpressure. At a given distance from the explosion, the time variation of the dynamic Pd behind the shock front is somewhat similar to that of the overpressure Ps, but the rate of decrease usually different. For design purposes, the negative phase of the overpressure in Fig.3.2 (b) is not important and can be ignored.

3.1.1 Explosive and impact loads similar to and different from loads typically used in building design.

Explosive loads and impact loads are transients, or loads that are applied dynamically as one-half cycle of high amplitude, short duration air blast or contact and energy transfer related pulse. This transient load is applied only for a specific and typically short period of time in

the case of blast loads, typically less than one-tenth of a second (Kirk A. Marchand, Farid Alfawakhiri (2005)). This means that an additional set of dynamic structural properties not typically considered by the designer, such as rate dependant material properties and inertial effects must be considered in design.

Often, design to resist blast, impact and other extraordinary loads must be thought of in the context of life safety, not in terms of serviceability or life-cycle performance. Performance criteria for other critical facilities (nuclear reactors, explosive and impact test facilities, etc.) may require serviceability and reuse, but most commercial office and industrial facilities will not have to perform to these levels. Structures designed to resist the effects of explosions and impact are permitted to contribute all of their resistance, both material linear and non-linear (elastic and inelastic), to absorb damage locally, so as to not compromise the integrity of the entire structure. It is likely that local failure can and may be designed to occur, due to the uncertainty associated with the loads.

3.2 EXPLOSIVE AIR BLAST LOADING

The threat for a conventional bomb is defined by two equally important elements, the bomb size, or charge weight *W,* and the standoff distance (*R)* between the blast source and the target (Fig.3.4). For example, the blast occurred at the basement of World Trade Centre in 1993 has the charge weight of 816.5 kg TNT. The Oklahoma bomb in 1995 has a charge weight of 1814 kg at a standoff of 5m . As terrorist attacks may range from the small letter bomb to the gigantic truck bomb as experienced in Oklahoma City, the mechanics of a conventional explosion and their effects on a target must be addressed.

Throughout the pressure-time profile, two main phases can be observed; portion above ambient is called positive phase of duration (*td*), while that below ambient is called negative phase of duration (*td*). The negative phase is of a longer duration and a lower intensity than the positive duration. As the stand-off distance increases, the duration of the positive-phase blast wave increases resulting in a lower-amplitude, longer-duration shock pulse. Charges situated extremely close to a target structure impose a highly impulsive, high intensity pressure load over a localized region of the structure; charges situated further away produce a lower-intensity, longer-duration uniform pressure distribution over the entire structure. Eventually, the entire structure is engulfed in the shock wave, with reflection and diffraction effects creating focusing and shadow zones in a complex pattern around the structure. During

the negative phase, the weakened structure may be subjected to impact by debris that may cause additional damage.

STAND-OFF DISTANCE

Stand-off distance refers to the direct, unobstructed distance between a weapon and its target.

HEIGHT OF BURST (HOB)

Height of burst refers to aerial attacks. It is the direct distance between the exploding weapon in the air and the target.

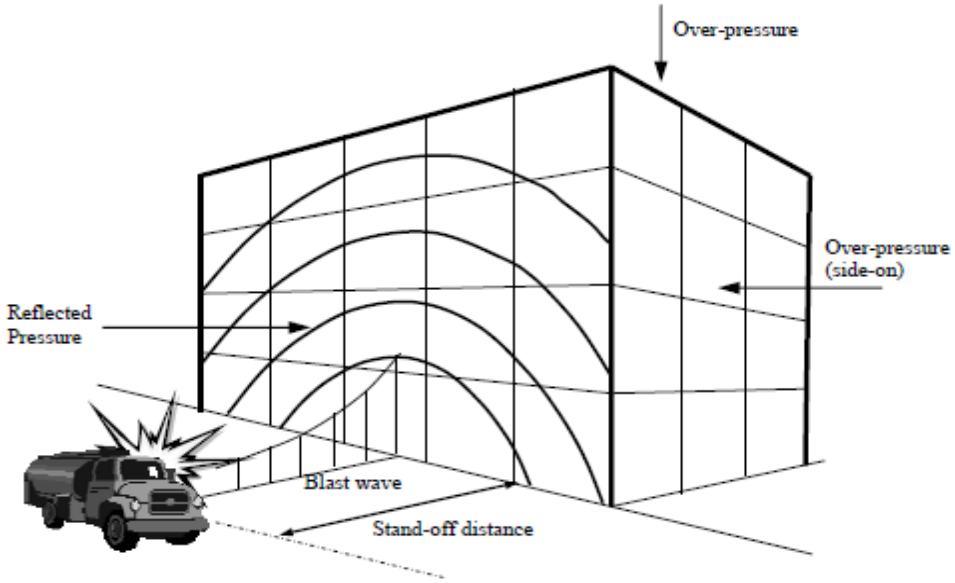

Figure 3.4: Blast Loads on a Building.

If the exterior building walls are capable of resisting the blast load, the shock front penetrates through window and door openings, subjecting the floors, ceilings, walls, contents, and people to sudden pressures and fragments from shattered windows, doors, etc. Building components not capable of resisting the blast wave will fracture and be further fragmented and moved by the dynamic pressure that immediately follows the shock front. Building contents and people will be displaced and tumbled in the direction of blast wave propagation. In this manner the blast will propagate through the building.

3.2.1 BLAST WAVE SCALING LAWS

All blast parameters are primarily dependent on the amount of energy released by a detonation in the form of a blast wave and the distance from the explosion. A universal normalized description of the blast effects can be given by scaling distance relative to $(E/Po)^{1/3}$ and scaling pressure relative to P_o, where E is the energy released (kJ) and P_o the

ambient pressure (typically 100 kN/m^2). For convenience, however, it is general practice to express the basic explosive input or charge weight *W* as an equivalent mass of TNT. Results are then given as a function of the dimensional distance parameter,

$$\text{Scaled Distance (Z)} = \frac{R}{W^{1/3}}$$

where, *R* is the actual effective distance from the explosion.
W is generally expressed in kilograms.

Scaling laws provide parametric correlations between a particular explosion and a standard charge of the same substance.

3.2.2 PREDICTION OF BLAST PRESSURE

Blast wave parameter for conventional high explosive materials have been the focus of a number of studies during the 1950's and 1960's. The estimations of peak overpressure due to spherical blast based on scaled distance $Z = \frac{R}{W^{1/3}}$ was introduced by Brode (1955) as:

$$P_{so} = \frac{6.7}{Z^3} + 1 \text{ bar} \qquad (P_{so} > 10 \text{ bar})$$

In 1961, Newmark and Hansen introduced a relationship to calculate the maximum blast pressure (Pso), in bars, for a high explosive charge detonates at the ground surface as: As the blast wave propagates through the atmosphere, the air behind the shock front is moving outward at lower velocity. The velocity of the air particles, and hence the wind pressure, depends on the peak overpressure of the blast wave. This later velocity of the air is associated with the dynamic pressure, $q(t)$.

3.3 STRUCTURAL RESPONSE TO BLAST LOADING

Complexity in analyzing the dynamic response of blast-loaded structures involves the effect of high strain rates, the non-linear inelastic material behaviour, the uncertainties of blast load calculations and the time-dependent deformations. Therefore, to simplify the analysis, a number of assumptions related to the response of structures and the loads has been proposed and widely accepted. To establish the principles of this analysis, the structure is idealized as a

single degree of freedom (SDOF) system and the link between the positive duration of the blast load and the natural period of vibration of the structure is established. This leads to blast load idealization and simplifies the classification of the blast loading regimes.

3.3.1 ELASTIC SDOF SYSTEMS

The simplest discretization of transient problems is by means of the SDOF approach. The actual structure can be replaced by an equivalent system of one concentrated mass and one weightless spring representing the resistance of the structure against deformation. The structural mass, *M*, is under the effect of an external force, *F*(*t*), and the structural resistance, *Rm*, is expressed in terms of the vertical displacement, *y*, and the spring constant, *K*. The blast load can also be idealized as a triangular pulse having a peak force *Fm* and positive phase duration *td* .

3.3.2 ELASTO-PLASTIC SDOF SYSTEMS

Structural elements are expected to undergo large inelastic deformation under blast load or high velocity impact. Exact analysis of dynamic response is then only possible by step-by-step numerical solution requiring nonlinear dynamic finite- element software. However, the degree of uncertainty in both the determination of the loading and the interpretation of acceptability of the resulting deformation is such that solution of a postulated equivalent ideal elasto-plastic SDOF system (Biggs, 1964) is commonly used. Interpretation is based on the required ductility factor $\mu = y_m/y_e$. For example, uniform simply supported beam has first mode shape $\varphi(x) = \sin \pi x/L$ and the equivalent mass $M = (1/2)\,mL$, where L is the span of the beam and m is mass per Unit length.

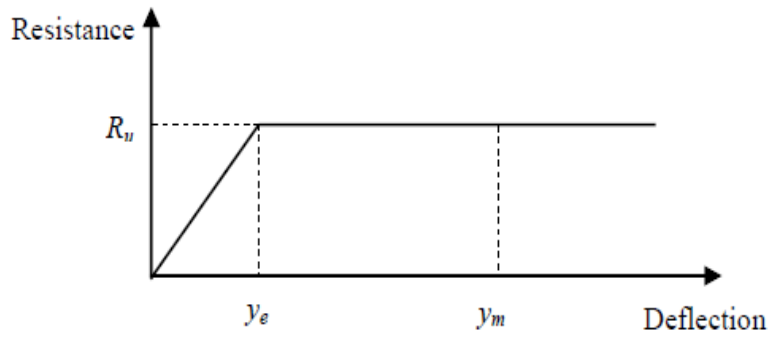

Figure 3.5 Simplified resistance function of an elasto-plastic SDOF system

The equivalent force corresponding to a uniformly distributed load of intensity p is $F = (2/\pi)pL$. The response of the ideal bilinear elasto-plastic system can be evaluated in

closed form for the triangular load pulse comprising rapid rise and linear decay, with maximum value F_m and duration t_d. The result for the maximum displacement is generally presented in chart form TM 5- 1300 (UFC 1990), as a family of curves for selected values of R_u/F_m showing the required ductility μ as a function of t_d/T, in which R_u is the structural resistance of the beam and T is the natural period (Figure 3.6).

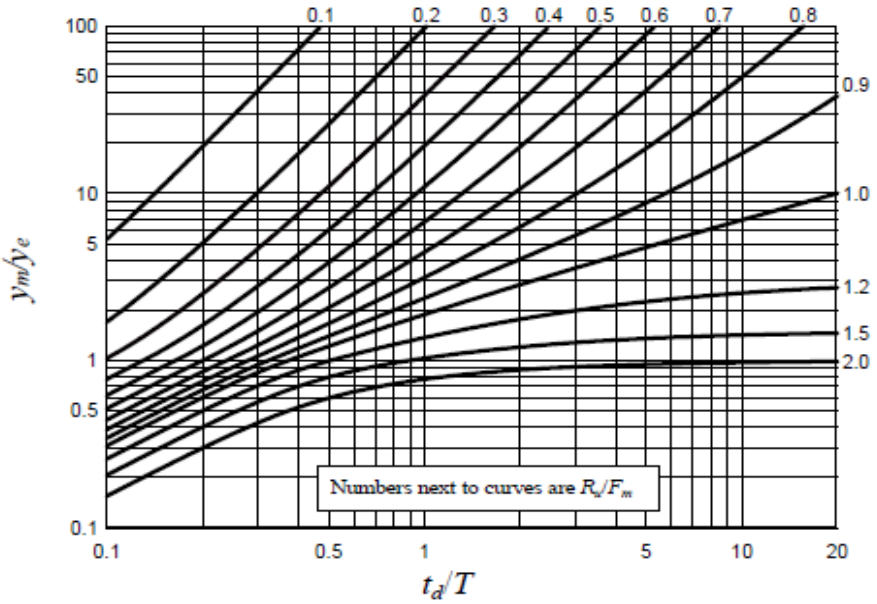

Figure 3.6 Maximum response of Elasto-plastic SDF system to a triangular load

3.4 MATERIAL BEHAVIORS AT HIGH STRAIN RATE

Blast loads typically produce very high strain rates in the range of $10^2 - 10^4\ s^{-1}$. This high loading rate would alter the dynamic mechanical properties of target structures and, accordingly, the expected damage mechanisms for various structural elements. For reinforced concrete structures subjected to blast effects the strength of concrete and steel reinforcing bars can increase significantly due to strain rate effects. Figure 3.7 shows the approximate ranges of the expected strain rates for different loading conditions. It can be seen that ordinary static strain rate is located in the range: $10^{-5}\text{to}\ 10^{-6}s^{-1}$, while blast pressures normally yield loads associated with strain rates in the range: $10^2{-}10^4\ s^{-1}$.

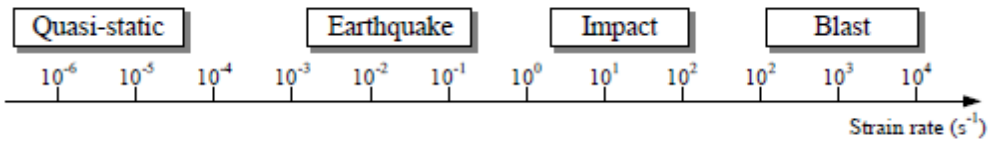

Figure 3.7 Strain rates associated with different types of loading

3.4.1 DYNAMIC PROPERTIES OF CONCRETE UNDER HIGH-STRAIN RATES

The mechanical properties of concrete under dynamic loading conditions can be quite different from that under static loading. While the dynamic stiffness does not vary a great deal from the static stiffness, the stresses that are sustained for a certain period of time under dynamic conditions may gain values that are remarkably higher than the static compressive strength (Figure 3.8). Strength magnification factors as high as 4 in compression and up to 6 in tension for strain rates in the range: $10^3 - 10^3$/sec have been reported (Grote et al., 2001).

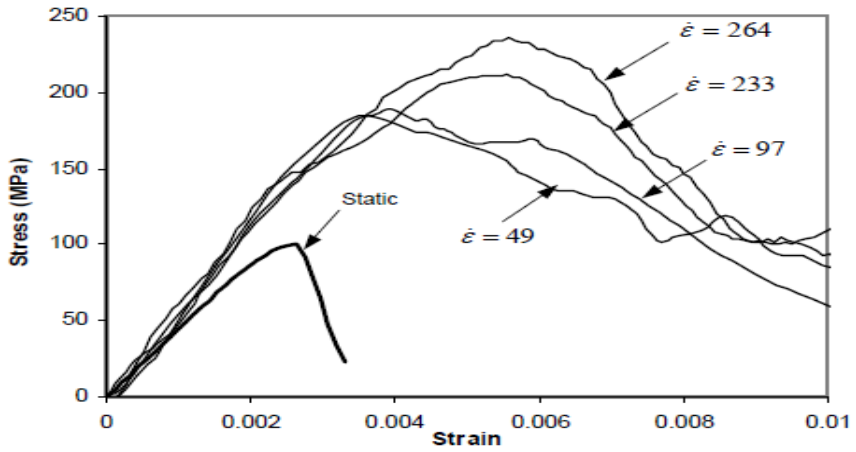

Figure 3.8 Stress-strain curves of concrete at different strain rates

3.4.2 DYNAMIC PROPERTIES OF REINFORCING STEEL UNDER HIGH-STRAIN RATES

Due to the isotropic properties of metallic materials, their elastic and inelastic response to dynamic loading can easily be monitored and assessed. Norris et al. (1959) tested steel with two different static yield strength of 330 MPa and 278 MPa under tension at strain rates ranging from 10^{-5} to 0.1/s (Norris et al., 1959). Strength increase of 9 - 21% and 10 - 23 % were observed for the two steel types, respectively. Dowling and Harding (1967) conducted tensile experiments using the tensile version of Split Hopkinton's Pressure Bar (SHPB) on mild steel using strain rates varying between 10^{-3} /s and 2000 /s. It was concluded from this test series that materials of bodycentered cubic (BCC) structure (such as mild steel) showed the greatest strain rate sensitivity. It has been found that the lower yield strength of mild steel can almost be doubled; the ultimate tensile strength can be increased by about 50%; and the upper yield strength can be considerably higher. In contrast, the ultimate tensile strain decreases with increasing strain rate. Malvar (1998) also studied strength enhancement of

steel reinforcing bars under the effect of high strain rates. This was described in terms of the dynamic increase factor (DIF), which can be evaluated.

CHAPTER 4

BLAT LOADING ON STEEL STRUCTURE

4.1 PROBLEM DESCRIPTION

The steel framed structure which has been considered for blast loading is taken from “Energy flow in progressive collapse of steel framed building” by Stefan Szyniszewski .This is a typical low rise steel building in the USA. All prevailing requirements for gravity, wind, and seismic design have been considered. It was designed for a typical office occupancy live load of 2.5 kPa. The floors were assumed to support a dead load of 4 kPa, which included a concrete-steel composite slab, steel decking, ceilings/ flooring/fireproofing, mechanical/electrical/plumbing systems and partitions (1 kPa). The framing plan of the investigated 3-story building is shown in Fig. 4.1, Column schedules and beam designation are given in Table 4.1 and Table 4.2, respectively, with designations in accordance with AISC .

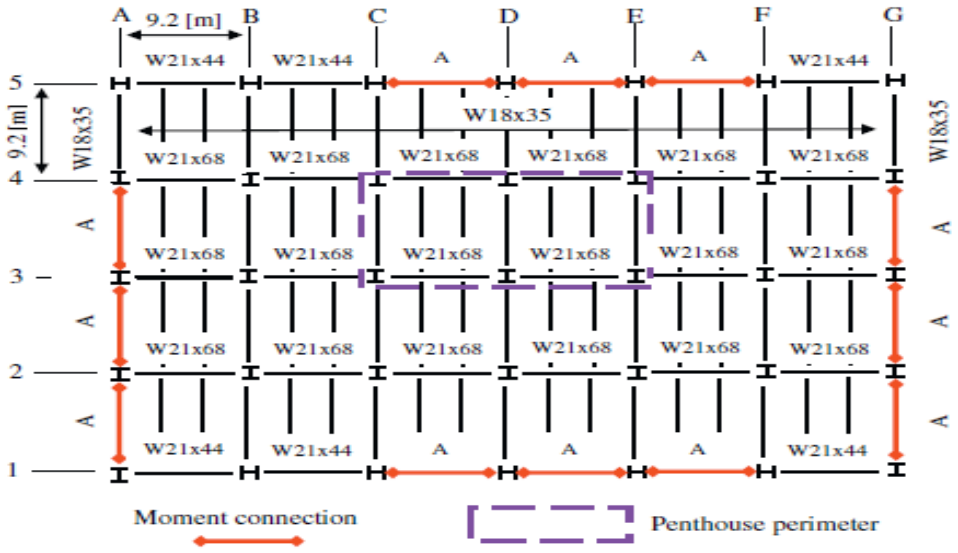

Fig 4.1 Framing plan of the representative steel building.

Table 4.1 Beam with moment resisting connection designated with “A”

Floor	2	3	Roof
Beam “A”	W18×35	W21×57	W21×62

Table 4.2 Steel Profile of Column

	A	B	C	D	E	F	G
5	W12×58	W12×58	W14×74	W14×99	W14×99	W14×74	W12×58
4	W14×74	W12×58	W12×65	W12×72	W12×65	W12×58	W14×74
3	W14×99	W12×58	W12×65	W12×72	W12×65	W12×58	W14×99
2	W14×99	W12×58	W12×58	W12×58	W12×58	W12×58	W14×99
1	W14×74	W12×58	W14×74	W14×99	W14×99	W14×74	W14×74

4.2 COMPUTATION OF BLAST PRESSURE

Peak Incident Pressure: The sudden increased value of the pressure on the surface due to an explosion resulting at a distance from the surface parallel to the propagation of the blast wave is called as the peak incident pressure. In Literature, various empirical relations are available to determine the pressure on the surface when the blast waves are unimpeded in its motion. Hence, the empirical relations available in literature to determine the peak incident pressure on a surface are as listed in the table below. Kinney and Graham (1985), based on the large experimental data provided the following relation to determine the peak pressure from an explosion.

Table 4.3 Peak Incident Pressure Calculation (Goel et al., 2012)

Kinney and Graham (1985)	$P_{pos} = P_0 \dfrac{808 \left[1+\left(\dfrac{Z}{4.5}\right)^2\right]}{\sqrt{\left[1+\left(\dfrac{Z}{0.048}\right)^2\right]\left[1+\left(\dfrac{Z}{0.32}\right)^2\left[1+\left(\dfrac{Z}{1.35}\right)^2\right]\right]}}$ (bar)
Sadovskiy (2004)	$P_{pos} = 0.085\left(\dfrac{W^{2/3}}{R}\right) + 0.3\left(\dfrac{W^{1/3}}{R}\right)^2 + 0.8\left(\dfrac{W^{1/3}}{R^2}\right)^3 (\text{MPa})$
Bajic (2007)	$P_{pos} = 1.02\left(\dfrac{W^{1/3}}{R}\right) + 4.36\left(\dfrac{W^{2/3}}{R}\right) + 14\left(\dfrac{W}{R^3}\right)$ (bar)
Brode (1955)	$P_{pos} = \dfrac{6.7}{Z^2} + 1\text{bar}\left(P_{Pos} \geq 10 \text{ bar}\right)$

Henrych (1979)	$P_{pos} = \frac{0.975}{Z} + \frac{1.455}{Z^2} + \frac{5.85}{Z^3} - 0.019 \qquad \left(0.1 \le P_{pos} \ge 10 \text{ bar}\right)$ $P_{pos} = \frac{6.194}{Z} + \frac{0.326}{Z^2} + \frac{2.132}{Z^3} \qquad \left(0.5 \le P_{pos} \le 1 \text{ bar}\right)$

Z = Scaled distance (m/kg$^{1/3}$)

R = Radial distance (m)

W = Charge weight (kg)

Positive time duration (t_{pos}): The time difference between passing of a wave front and the end of the positive pressure phase marked by the passing of zero pressure point at a particular surface is called as the positive time duration (t_{pos}) of the blast wave. The positive time duration of a blast wave on any surface depends on the dissipation of the waves around that surface. If the surface is of small size, the positive time duration will be less as compared to a larger surface as the time required to surpass the surface will be more, hence, less dissipation possible. Many empirical relations are available in the literature to calculate the positive time duration of an explosion based on the scaled distance.

Table 4.4 Positive Time Duration (Goel et al., 2012)

Kinney and Graham (1985)	$t_{pos} = W^{1/3} \dfrac{980 \quad \left[1 + \left(\frac{Z}{0.45}\right)^{10}\right]}{\left[1 + \left(\frac{Z}{0.02}\right)^{3} \times \left[1 + \left(\frac{Z}{0.74}\right)^{6}\right]\right] \sqrt{\left[1 + \left(\frac{Z}{6.9}\right)^{2}\right]}}$ (msec)
Henrych (1979)	$t_{pos} = 10^{(-2.75 + 0.27 \log_{10} Z) + \log_{10} W^{1/3}}$ (msec)

Positive Impulse (I_{pos}): The area under the pressure-time history curve is called as impulse. The peak pressure decreases rapidly from the highest value to zero, described as quasi-exponential decrease. For simplicity, this decrease in the value of the peak pressure can be considered as

triangular, rectangular keeping the impulse constant. The following are the empirical relations available for calculating the impulse of a wave pressure wave.

Table 4.5 Positive Impulse (Goel et al., 2012)

Kinney and Graham (1985)	$I_{pos} = \frac{0.067\sqrt{\left[1+\left(\frac{Z}{0.23}\right)^4\right]}}{Z^2\sqrt[3]{1+\left(\frac{Z}{1.55}\right)^3}}$ (bar – ms)
Held (1983)	$I_{pos} = 300\frac{W^{2/3}}{R}$ (Pa – sec)
Sadovskiy (2004)	$I_{pos} = 200\frac{W^{2/3}}{R}$ (Pa – sec)

4.3 FRIEDLANDER'S WAVEFORM

The quasi-exponential decay of the blast pressure can be explained and represented with the help of Friedlander's equation. The basic equation is given as,

$$P(t) = P_{pos}\left(1-\frac{t}{t_{pos}}\right)e^{\frac{t}{t_{pos}}} \quad (4.1)$$

however, the equation was later modified and called as the modified Friedlander's equation.

$$P(t) = P_{pos}\left(1-\frac{t}{t_{pos}}\right)e^{\frac{-b(t-t_A)}{t_{pos}}} \quad (4.2)$$

where $P(t)$ is pressure at any time t, P_{pos} is peak positive pressure, t_{pos} is positive time duration, and b is wave decay parameter.

The wave-decay parameter b describes the decay in the pressure at any time t after the arrival of the pressure wave on the surface of the structure. The other parameters for the pressure time history can be found with the help of empirical relations explained earlier. Later, Lam et al. (2004) used ratio of under pressure with positive pressure to compute the wave-decay parameter (b) and reported the following relation of b with scaled distance.

$$b = Z^2 - 3.7Z + 4.2$$

With the help of the previously explained parameters in this chapter, the incident pressure time history parameters can be found for a particular TNT explosion at a specific radial distance for a specified charge weight. The resulting pressure on the structure from an explosion is higher than the incident pressure and called as the reflected pressure. The peak reflected pressure of an explosion will be nearly 2.5 to 3.4 times the peak incident pressure (Gebbeken et al., 2010). As per G. C. Mays (1995), the reflected time history positive phase duration will be same as the incident time history positive phase if the pressure waves are totally reflected back without any dissipation around the structure but the difference in the values are very small, hence, neglected. The positive phase duration of the blast waves depends on the area of the structure exposed to the blast loads. To find the reflected pressure time history parameters, the following approach is used with UFC 3-340-02.

4.4 PEAK REFLECTED PRESSURE (P_{ref})

When a pressure wave generated from an explosion impinge a surface at an angle, it is reflected, which results in higher pressure on the surface than the incident side-on pressure. The magnitude of the reflected pressure depends on the angle of incidence of the blast wave, the radial distance of the detonation point from the surface, peak incident pressure developed due to the explosion, the type of pressure wave, and the properties of the surface. The magnitude of the reflected pressure is generally determined from the coefficient of reflection,

$$P_{ref} = C_r P_{pos}$$

Where C_r = Coefficient of reflection.

UFC 3-340-02 gives the detailed procedure of determining the peak reflected pressure on a surface depending upon the peak incident pressure and angle of incidence of the waves. Figure 3.3 shows the coefficient of reflection (C_r) based on the peak incident pressure of the explosion and the angle of incidence of the blast wave at a particular point on the surface. The angle of incidence varies from 0° (wave parallel to the surface) to 90° (wave perpendicular to the surface) with the peak incident pressure.

4.5 PRESENT APPROACH

Based on the earlier described parameters defining the blast pressure time history function, in the present approach to find out the peak pressures at the different joint of the structure resulting from an explosion, the following approach is adopted.

i. The unimpeded peak blast pressures resulting from an explosion at different radial

distance are computed by using the empirical relations given by Kinney and Graham (1985). The empirical relation are based on the scaled distance (Z) in $\mathrm{m}/\mathrm{kg}^{1/3}$ which itself depends on the charge weight (W) in kg and radial distance (R) in m.

ii. To find out the incident pressure duration, Kinney and Graham's (1985) empirical relations reported in Goel et al. (2012) are used. The positive phase durations (t_{pos}) are based on the scaled distance (Z) in $\mathrm{m}/\mathrm{kg}^{1/3}$.

iii. To find out the peak reflected pressure on the building at different joints resulting from an explosion, the coefficient of reflections are computed based on the peak incident pressure and the angle of incidence of the blast waves from Figure 3.3. The angle of incidence is defined as the angle made by the blast wave propagating towards the surface of the structure with its normal.

iv. The reflected positive phase duration is taken equal to the duration of the incident positive pressure phase, as the difference is very small. The negative phase of the pressure time history is neglected in the present approach.

v. The distributions of the blast pressure from the walls to the joints are taken as given in the Figure 3.4. The structures are analyzed by considering only the peak pressure are acting on the joints and the detonation points to be in front of different faces of the buildings based on column orientations (I-section).

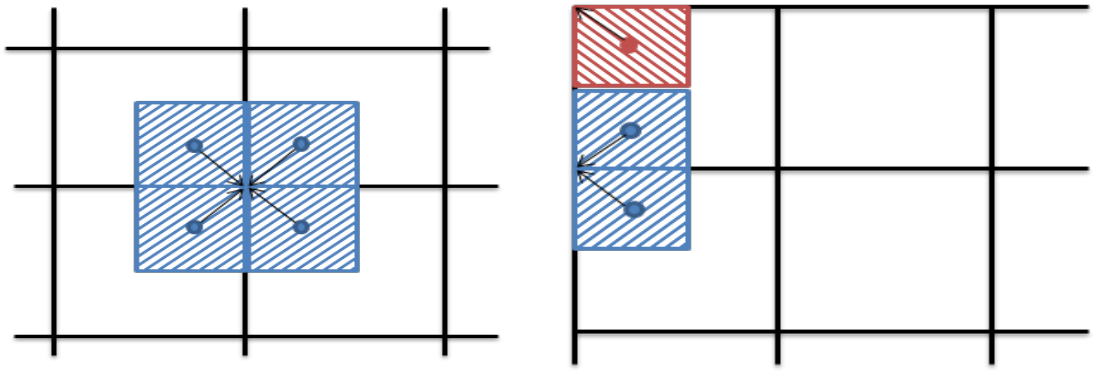

Figure 4.2 Distribution of Blast Pressure from Walls to the Joints

4.6 RESULTS

Blast pressures have been computed according to the procedure discussed above. Then, the loads computed have been applied on the joints facing the blast site. The modeling has been

done in CSI SAP2000® program. The results in terms of certain response parameters are presented here.

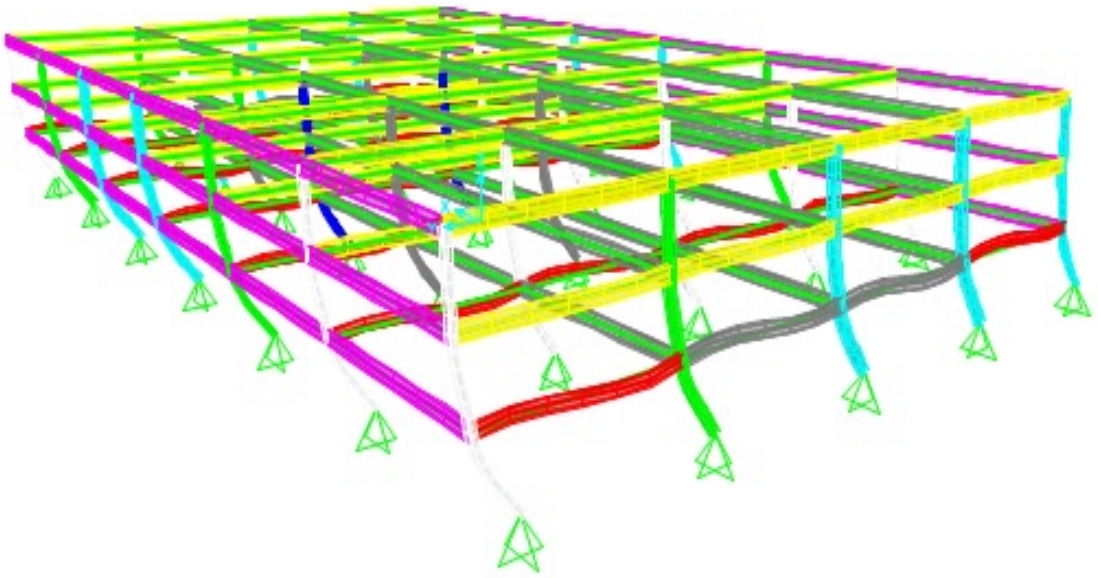

Fig 4.3 Deflection of Steel structure

JOINT REACTIONS

The joint reactions and joint displacements results is obtain after the analysis in SAP 2000 and it shows that the reactions and displacements are quite large that may cause the total collapse of steel structure in shear. Results are obtained in Excel file as internally generated after the analysis is shown in Table 4.6

Table 4.6 Joint Displacements Due to DL and LL

TABLE: Joint Displacements								
Joint	OutputCase	CaseType	U1	U2	U3	R1	R2	R3
Text	Text	Text	m	m	m	Radians	Radians	Radians
1	DEAD	LinStatic	0	0	0	-0.00014	7.05E-06	-2.4E-06
1	LIVE	LinStatic	0	0	0	-0.31557	-0.0047	-0.00056
2	DEAD	LinStatic	-6.9E-05	0.000013	-0.00169	0.000267	-8.9E-05	-2.4E-06
2	LIVE	LinStatic	-0.01031	0.661753	0.00009	-0.02982	-0.00067	-0.00056
3	DEAD	LinStatic	-0.0001	0.000036	-0.00282	0.000377	-0.00021	-3E-06
3	LIVE	LinStatic	-0.0147	0.896236	0.000153	-0.00167	-0.00045	-0.0008
4	DEAD	LinStatic	-0.00014	0.000052	-0.00338	0.00037	-0.0002	-4.8E-06
4	LIVE	LinStatic	-0.0165	0.965126	0.000085	0.001217	-0.00033	-0.00092
5	DEAD	LinStatic	0	0	0	-6.5E-06	-0.00011	-2.8E-06
5	LIVE	LinStatic	0	0	0	-0.26499	-0.00259	-0.00045

6	DEAD	LinStatic	-4.8E-05	0.000014	-0.00081	7.9E-08	0.00017	-2.8E-06
6	LIVE	LinStatic	-0.00535	0.659747	0.00159	-0.09994	-0.00012	-0.00045
7	DEAD	LinStatic	-7.4E-05	0.000037	-0.00136	0.000019	0.000212	-3.4E-06
7	LIVE	LinStatic	-0.00726	0.894628	0.001989	-0.02965	0.000242	-0.00079
8	DEAD	LinStatic	-9.8E-05	0.00005	-0.00163	0.000035	0.000386	-3.9E-06
8	LIVE	LinStatic	-0.00797	0.96436	0.002024	-0.00866	0.000464	-0.00092
9	DEAD	LinStatic	0	0	0	-2.2E-06	-8.6E-05	-3.2E-06
9	LIVE	LinStatic	0	0	0	-0.27394	0.000103	-0.0006
10	DEAD	LinStatic	-0.00002	0.000014	-0.0008	-1.2E-05	0.000157	-3.2E-06
10	LIVE	LinStatic	0.000234	0.659172	-0.00085	-0.0754	0.000027	-0.0006
11	DEAD	LinStatic	-4.3E-05	0.000036	-0.00133	-2.8E-05	0.000196	-3.3E-06
11	LIVE	LinStatic	0.000384	0.893284	-0.00116	-0.02646	-4.8E-05	-0.00077
12	DEAD	LinStatic	-6.5E-05	0.00005	-0.0016	-4.9E-05	0.000391	-3.4E-06
12	LIVE	LinStatic	0.000606	0.963735	-0.00128	-0.00657	0.00003	-0.00091
13	DEAD	LinStatic	0	0	0	-2.6E-06	-0.00013	-2.9E-06
13	LIVE	LinStatic	0	0	0	-0.27241	0.002853	-0.00053
14	DEAD	LinStatic	8.97E-06	0.000015	-0.00107	-1.1E-05	0.000264	-2.9E-06
14	LIVE	LinStatic	0.006048	0.658958	-0.00178	-0.08846	0.000314	-0.00053
15	DEAD	LinStatic	-1.1E-05	0.000037	-0.00178	-0.00002	0.000299	-3.5E-06
15	LIVE	LinStatic	0.008086	0.892958	-0.00235	-0.02589	0.000025	-0.0008
16	DEAD	LinStatic	-3.6E-05	0.000049	-0.00214	-2.7E-06	0.000467	-3.5E-06
16	LIVE	LinStatic	0.009177	0.963439	-0.00254	-0.00721	-4.3E-05	-0.00091
17	DEAD	LinStatic	0	0	0	3.28E-06	4.51E-06	-3E-06
17	LIVE	LinStatic	0	0	0	-0.29797	0.004975	-0.00063
18	DEAD	LinStatic	0.000037	0.000015	-0.00068	-2.2E-05	0.000031	-3E-06
19	DEAD	LinStatic	0.000019	0.000037	-0.00113	0.000032	0.000011	-3.1E-06
19	LIVE	LinStatic	0.015541	0.892892	-0.00195	-0.01254	0.000439	-0.00078
20	DEAD	LinStatic	-2.6E-06	0.000049	-0.00136	0.000093	0.000075	-3.8E-06
20	LIVE	LinStatic	0.017603	0.963347	-0.00212	-0.00276	0.000283	-0.00091
21	DEAD	LinStatic	0	0	0	0.00007	-1.8E-05	-2.9E-06
21	LIVE	LinStatic	0	0	0	-0.30189	-0.00473	-0.00051
22	DEAD	LinStatic	-7.1E-05	-1.3E-05	-0.00136	-0.00013	-3.7E-05	-2.9E-06
22	LIVE	LinStatic	-0.01031	0.657188	0.000578	-0.05059	-0.00033	-0.00051
23	DEAD	LinStatic	-0.0001	5.23E-06	-0.00227	-0.00025	-5.3E-05	-3.5E-06
23	LIVE	LinStatic	-0.01455	0.888986	0.000746	-0.01206	-0.00017	-0.0008
24	DEAD	LinStatic	-0.00014	0.000017	-0.00273	-0.00038	-5.1E-05	-3.6E-06
24	LIVE	LinStatic	-0.01641	0.956684	0.000693	-0.00276	-1.9E-06	-0.00092
25	DEAD	LinStatic	0	0	0	0.00002	-0.00008	-3E-06
25	LIVE	LinStatic	0	0	0	-0.27272	-0.00271	-0.00056
26	DEAD	LinStatic	-4.5E-05	-1.3E-05	-0.00264	-3.3E-05	0.000117	-3E-06
26	LIVE	LinStatic	-0.0052	0.65574	-0.00104	-0.08794	0.00026	-0.00056

Table 4.7 Joint Reactions due to DL and LL

TABLE: Joint Reactions					
Joint	OutputCase	CaseType	F1	F2	F3
Text	Text	Text	KN	KN	KN
1	DEAD	LinStatic	-0.28	-0.06	481.629
1	LIVE	LinStatic	11.766	-41.915	-25.578
5	DEAD	LinStatic	2.055	-0.135	1017.81
5	LIVE	LinStatic	18.376	-3388.27	-1989.96
9	DEAD	LinStatic	1.805	0.198	1003.934
9	LIVE	LinStatic	-0.568	-4075.77	1059.189
13	DEAD	LinStatic	0.964	0.122	1001.559
13	LIVE	LinStatic	-6.293	-2708	1670.657
17	DEAD	LinStatic	0.232	0.05	496.605
17	LIVE	LinStatic	-33.322	-469.668	982.183
21	DEAD	LinStatic	-0.166	0.396	996.965
21	LIVE	LinStatic	38.67	-497.301	-422.656
25	DEAD	LinStatic	0.389	0.461	1927.595
25	LIVE	LinStatic	5.883	-1623.26	758.949
29	DEAD	LinStatic	0.372	-0.04	1930.156
29	LIVE	LinStatic	-0.564	-1716.95	619.44
33	DEAD	LinStatic	-0.103	-0.339	1932.07
33	LIVE	LinStatic	-5.32	-1644.58	1251.349
37	DEAD	LinStatic	0.193	-0.287	987.793
37	LIVE	LinStatic	-47.966	-451.591	1167.597
41	DEAD	LinStatic	0.326	0.694	978.325
41	LIVE	LinStatic	61.394	-568.159	-466.39
45	DEAD	LinStatic	-0.106	0.461	1948.677
45	LIVE	LinStatic	3.929	-1651.26	737.106
49	DEAD	LinStatic	-0.455	-0.302	1954.816
49	LIVE	LinStatic	-0.385	-1901.44	665.099
53	DEAD	LinStatic	0.301	-0.183	1968.22
53	LIVE	LinStatic	-9.976	-1808.3	1209.269
57	DEAD	LinStatic	-1.103	-0.242	973.904
57	LIVE	LinStatic	-66.527	-538.589	1241.501
61	DEAD	LinStatic	0.402	1.496	1008.272
61	LIVE	LinStatic	85.084	-1400	-1142.34
65	DEAD	LinStatic	0.066	0.86	1766.431
65	LIVE	LinStatic	5.653	-1794.07	1509.129
69	DEAD	LinStatic	0.144	-0.663	1807.412
69	LIVE	LinStatic	-2.109	-1954.48	388.611
73	DEAD	LinStatic	-0.894	-0.021	1907.777
73	LIVE	LinStatic	-9.76	-2178.45	571.095
77	DEAD	LinStatic	0.321	0.201	1013.229

CHAPTER 5

BLAST SIMULATION USING ANSYS AUTODYN®

5.1 INTRODUCTION

ANSYS Autodyn® software is a versatile explicit analysis tool for modeling the nonlinear dynamics of solids, fluids, gases and their interactions. The product has been developed to provide advanced capabilities within a robust, easy-to-use software tool. Simulation projects can be completed with significantly less effort, less time and lower labor costs than with other explicit programs. This high productivity is a result of the quick-to-learn, intuitive, interactive graphical interface implemented. Time and effort are saved in problem setup and analysis by automatic options to define contact, by coupling interfaces and by minimizing input requirements using safe logical defaults. This chapter describes the simulation of blast load on structure with basic explanation on material models, explosives modeling for planar and 3D parts using different solvers.

In this chapter, an example of a column of single storey steel moment frame and a concrete wall with or without steel plate is presented, which is subjected to blast pressure emanating from TNT charge placed above ground level. Different response parameters including the variation in blast overpressure is obtained. The simulation is done using Autodyn.

5.2 EXPLICIT DYNAMIC MODEL

In general, materials have a complex response to dynamic loading and the phenomena may need to be modeled are non-linear pressure, strain hardening, strain rate hardening, thermal softening, compaction, crushing damage, chemical energy decomposition (explosives) and tensile failure. The modeling of such phenomenon are broken into three components

5.3 EQUATION OF STATE

An equation of state describes the hydrodynamic response of a material. This is the primary response for gases and liquids, which can sustain no shear. Their response to dynamic loading is assumed hydrodynamic, with pressure varying as a function of density and internal energy. This is also the primary response for solids at high deformation rates, when the hydrodynamic pressure is far greater than the yield stress of the material.

***JWL equation of state*:** The JWL equation of state describes the detonation product expansion down to a pressure of 1 kbar for high energy explosive materials. It has been proposed by Jones, Wilkins and Lee according to following equation

$$p = A\left(1 - \frac{w\eta}{R_1}\right)e^{\frac{-R_1}{\eta}} + B\left(1 - \frac{w\eta}{R_2}\right)e^{\frac{-R_1}{\eta}} + w\rho e$$

where ρ_0 is reference density, ρ density and $\eta = \rho/\rho_0$

The values of the constants *A, B, R1, R_2 and ω* for many common explosives have been determined from dynamic experiments.

The standard JWL equation of state can be used in combination with an energy release extension whereby additional energy is deposited over a user-defined time interval. Thermo baric explosives show this behavior and produce more explosive energy than conventional high energy explosives through combustion of inclusions, like aluminum, with atmospheric oxygen after detonation.

5.3.1 Material strength model

Solid materials may initially respond elastically, but under highly dynamic loadings, they can reach stress states that exceed their yield stress and deform plastically. Material strength laws describe this non-linear elastic-plastic response.

5.3.2 Material failure model

Solids usually fail under extreme loading conditions, resulting in crushed or cracked material. Material failure models simulate the various ways in which materials fail. Liquids will also fail in tension, a phenomenon usually referred to as cavitation.Ansys Autodyne provides extensive set of engineering material data in its library.

5.4 PARTS CREATION

In AUTODYN®, model is built using parts. The parts can structured or unstructured. For structured parts in AUTODYN®, all information relating to the mesh and the elements in the mesh are stored and processed using the concept of I, J and K lines (IJK-space). For unstructured parts an alternative "Unstructured" approach to storing and processing information relating to the mesh is used for the solvers. The basic entities needed in the simulation are the Nodes, Elements, Faces, and Joints and so on.

5.5 PLANAR DETONATION

The part is modelled using 2D Euler multi material solver creating wedge shape geometry with required zoning grids. The part is filled with air first, then in same part TNT is filled with geometric fill option. Location of explosives to be detonated is set using detonation point. The model is run for required time to obtain output parameters like pressure.

The 2D detonation can be remapped in 3D using option available under Part>Fill>Additional fill>data map/read.

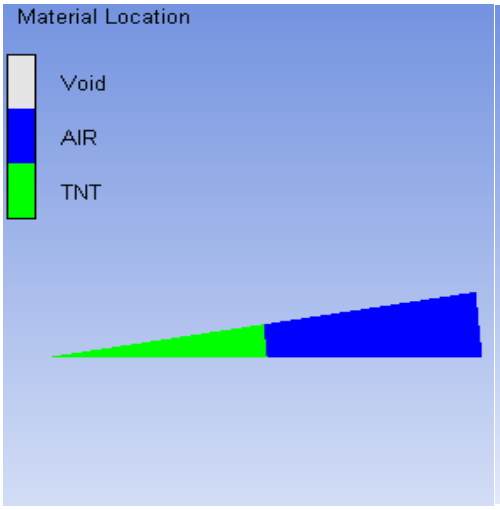

Fig. 5.1 TNT filled in Air

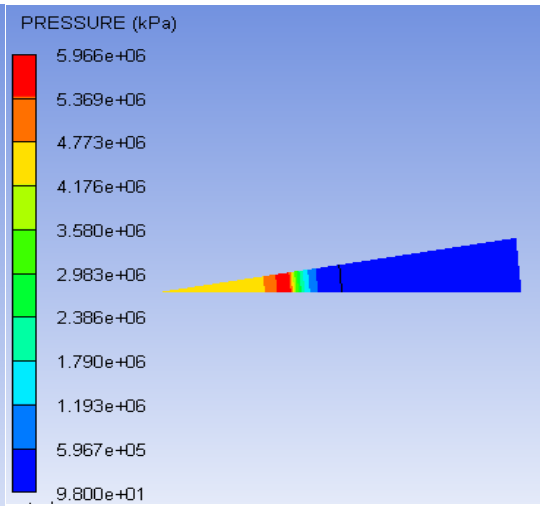

Fig. 5.2 Pressure contours

5.6 AUTODYN BLAST SIMULATIONS

5.6.1 Modelling/ Methodology

Geometry modelling: The 3D solid geometry of steel column and wall sections are modelled using geometry module in Ansys Explicit dynamic which is then transfferd to Ansys Autodyn envirnoment using Design Modeler component maintaining units consistancy, i.e., in meters.

Workbench Project Schematic: In workbench the project flow is created using analysis systems and components in project schematic window. From analysis system Explicit Dynamics module is launch and interconnection is made to component Autodyn as shown in Figure 5.3.

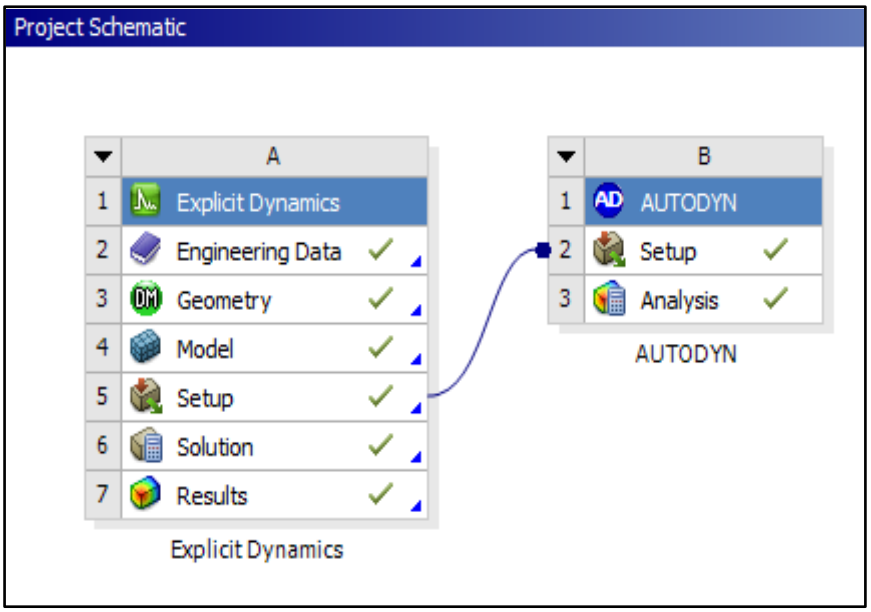

Fig 5.3 Workbench project schematic

FE Modeler: The model imported from design modeler is transferred to workbench which then attach to FE modeler for meshing and analysis. The model is meshed using tetrahedron element with lagrangian setting using finer mesh. The fixed boundary are applied to bottom surfaces of columns and walls. Model is set with intial condition i.e. zero velocities are applied. Superstructure load is estimated and applied as uniformely distributed load on beams and point load on columns. The standard gravity load is applied to model. The analysis is run for 1second and workbench envirnoment is updated for exporting upstream data to Autodyn.

Autodyn Blast Simulation: Imported data from workbench i.e. steel frame structure is assigned the gauge points to record data of output parameters, also material is reassign or modified to define strength and failure parameters.

Air medium modeling

Air medium is created using 3D Euler multimaterial fill part with suitable geometry and zoning. The part is entirely filled with air material defining the density and internal energy. The air medium is assign the flow out boundary condition which is best suited for explosive.

Explosive modelling

There are two ways to model explosives in Autodyn using TNT or PETN as material with equation of state as JWL. The standard density of above material is known from which the required charge weight is figured out as equivalent radius of volume of sphere.

(a) Explosive defined using grid fill

In this approch explosive is filled in 3D Euler multimaterial part using block fill or fill by suitable geometry option at required location i.e. standoff distance. The detonation or deflagration is defined for explosives defining detonation time and geometry option.

(b) Explosive defined using remap

In this, explosive is modeled using separate file taking advantage of axial symmetry using 2D Euler multimaterial part with wedge shape geometry as air medium. This part is filled using geometic fill ellipse option to fill explosive material of equvalent radius to achieved required charge weight. This is mapped using datafill write option under parts>fill>additional fill >data write.

This file is remap in 3D by accessing file under parts>fill>additional fill >data>read. Standoff distance is obtain by specifying location of remap.

Lagrange-Euler interaction

Interaction is set between different part using lagrange-Euler interaction as unstructured part is assigned lagrange solver and air medium with Euler. This is defined as fully coupled with defining ambient pressure and setting control to automatic as no shell part is present in structure.

Analysis control

Analysis options are set by defining wrap up time and cycles. There many option in this like setting time step and time increment, erosion set, cutoff settings.

Solving and post processing

The analysis is run for specified time and cycles to obtain output parameters like preesure, displacement, strain, stress and so on which then plotted using history graph. The material status, contours are plotted on structure under plot title.

Limitations

There are few limitations observed in pre processing as well as post processing. The failure of structure can be defined using material failure model but failure definition from serviceability limits was not seen. The text output file of analysis option was available, but the written file is not reflected in directory.

5.7 BLAST LOADING OF A COLUMN

A ground floor column of a multi-storey building is analyzed in this study. It is assumed that this column is vulnerable to blast lading being located at the ground floor. The properties of the column are given in Table 5.1. The blast pressure coming from different values charge weights of TNT are considered with different positions (standoff distances) of the blast points relative to the column. The blast load was calculated by using Kinney and Graham's approach for stand-off distances of 3 m, 4 m and 5 m with TNT charge weights of 20kg, 50kg and 100kg of TNT. This approach which is based on the large experimental data provided the following relation to determine the peak pressure from an explosion. The 3D model of a column (Fig 5.4a) was analyzed using ANSYS Explicit Dynamics. The effect of the blast loading was modeled in the dynamic analysis to obtain the total deflection, stress and strain in the column.

Table-5.1: Steel column properties

Area of cross section (m^2)	16.7
Overall Depth (in)	21.06
Width of flange (in)	6.55
Thickness of flange (in)	0.65
Thickness of web (in)	0.405
Moment of Inertia about string axis (in^4)	1170
Height of steel section (in)	197
Mass Density (kg/m^3)	7830

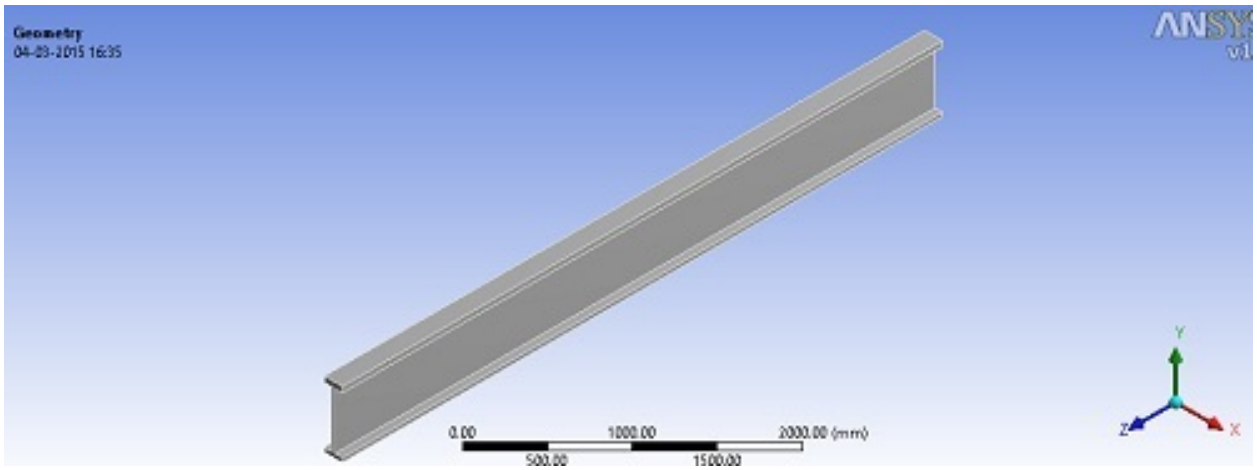

Fig 5.4 a) Geometric Model of Steel Colum in ANSYS/Autodyne.

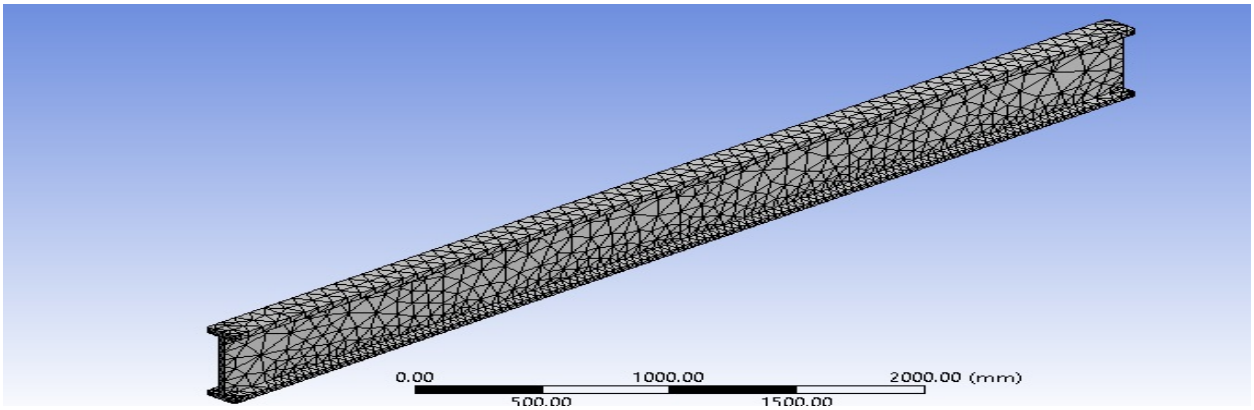

Fig 5.4 b) CFX Meshing of Steel Column

5.8 RESULTS

The response of the column in terms of net maximum deformation and maximum principal stress developed is obtained for different stand-off distances and charge weights. The results are tabulated as shown below:

Table 5.2 Response of Column Due to Charge Weight 20 Kg TNT

STAND-OFF DISTANCE	**3m**	**4m**	**5m**
TOTAL DEFORMATION (MM)	0.86	0.3507	0.2946

MAX. PRINCIPAL STRESS (Mpa)	56	19.787	12.891
MAX. PRINCIPAL ELASTIC STRAIN (mm/mm)	1.93e-03	1.05e-05	6.86e-05

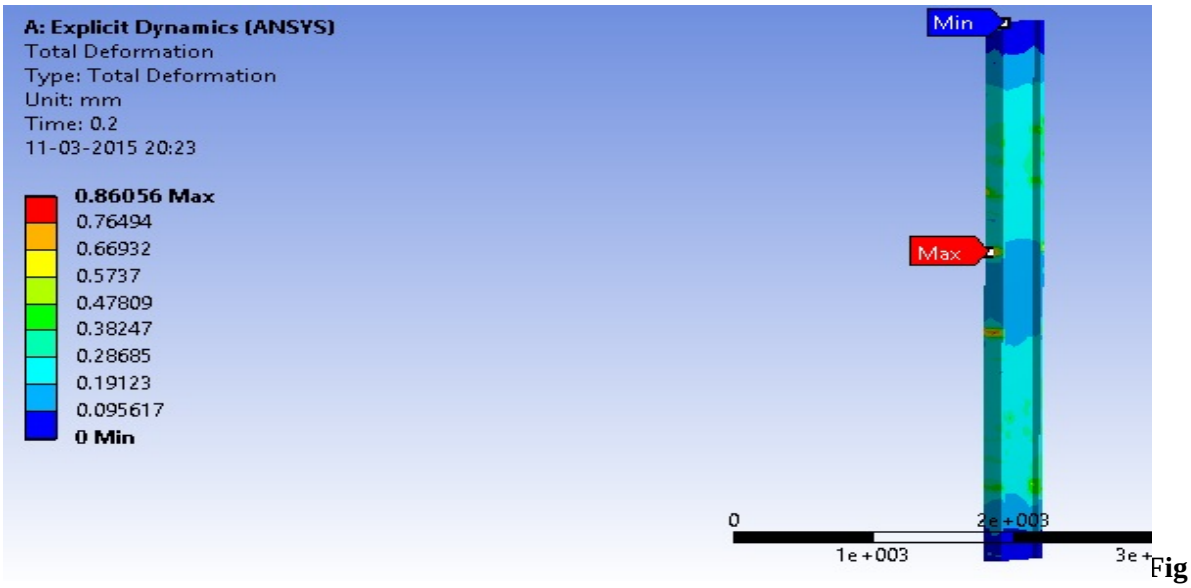

Fig

5.5 a) Maximum Deformation

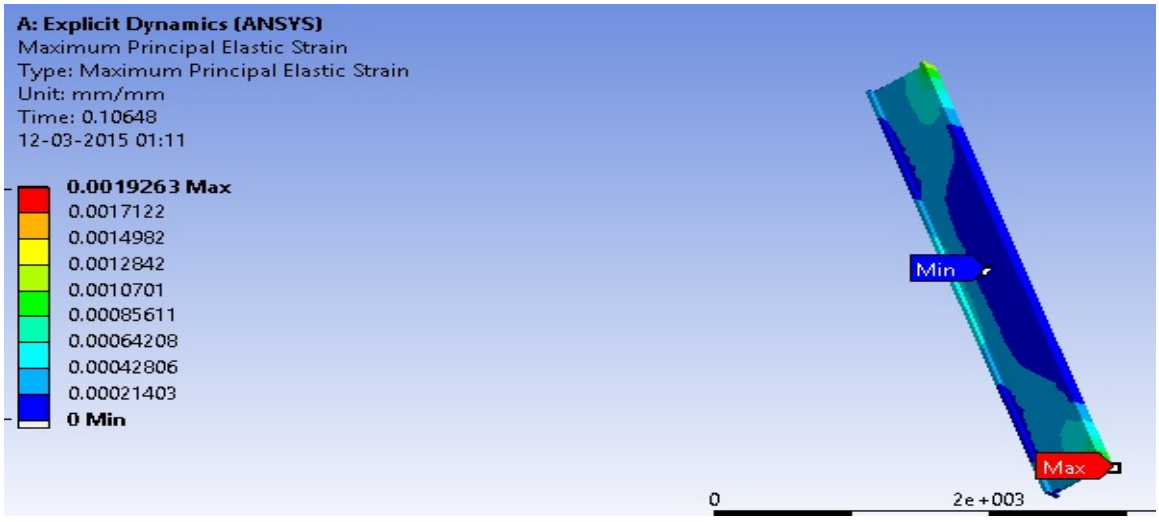

Fig 5.5 b) Maximum Principal Elastic stress

Table 5.3 Response Of Column Due to Charge Weight 50 Kg TNT

STAND-OFF DISTANCE	3m	4m	5m
TOTAL DEFORMATION (mm)	2.085	0.86441	0.6118
MAX. PRINCIPAL STRESS (Mpa)	114.73	50.026	32.993
MAX. PRINCIPAL ELASTIC STRAIN (mm/mm)	6.06E-004	2.065E-004	1.75E-004

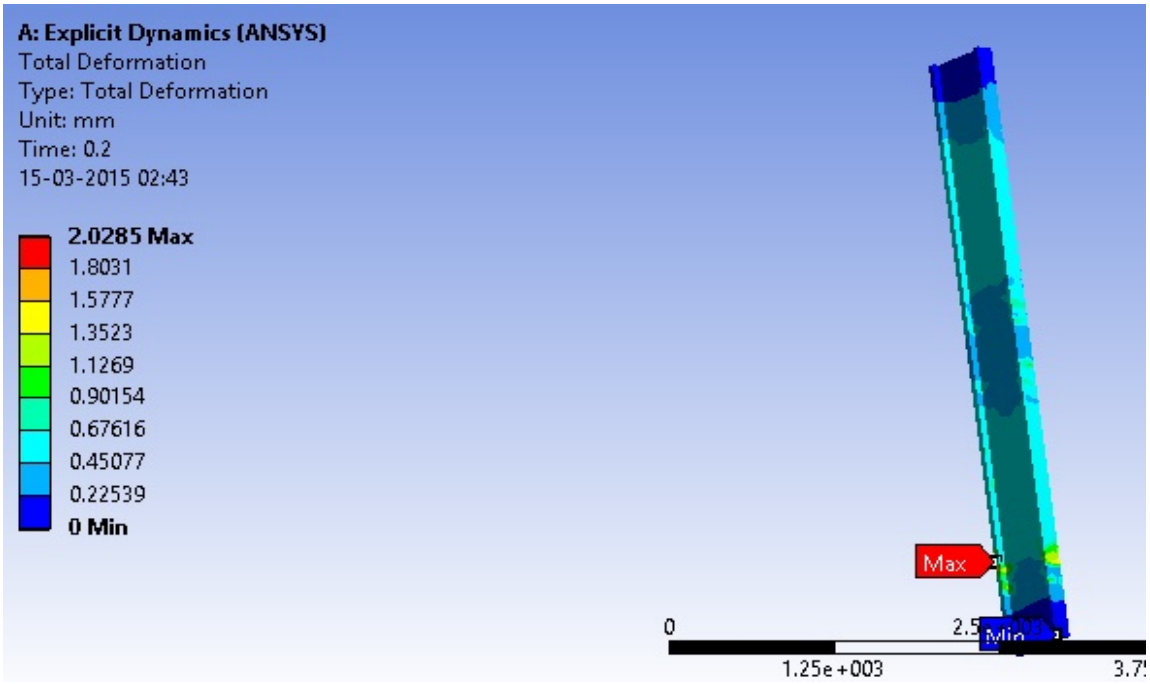

Fig 5.6 a) Maximum Deformation

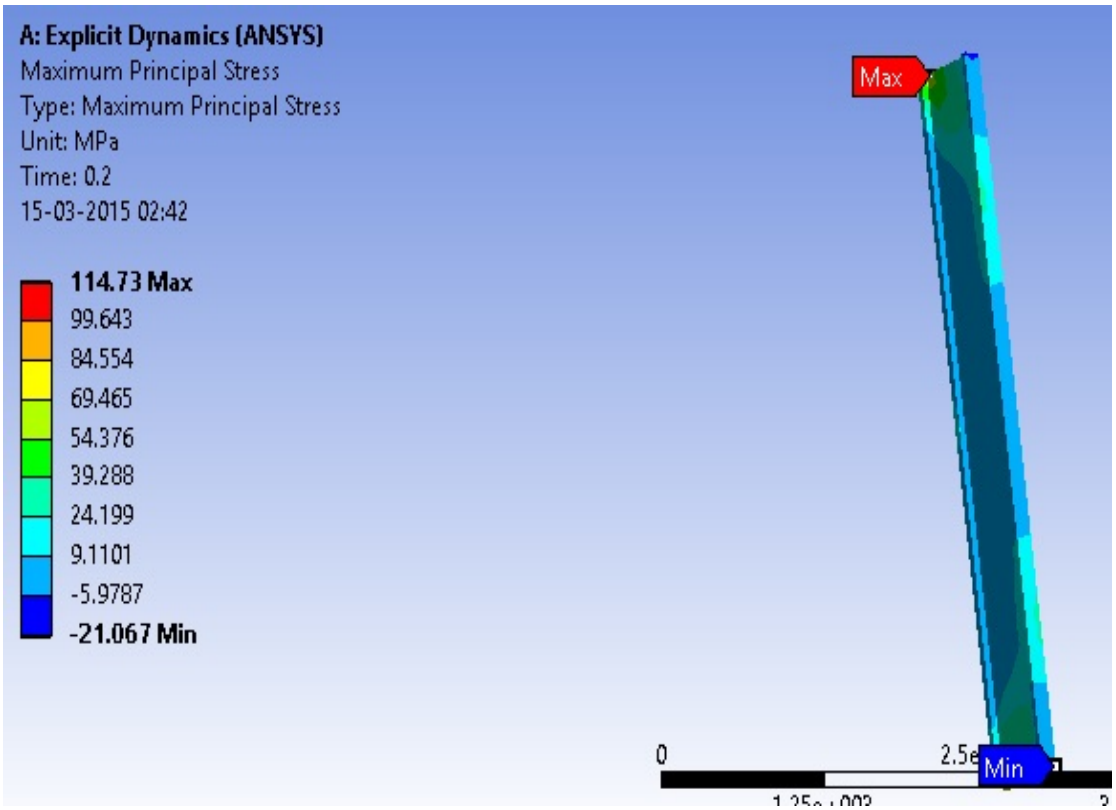

Fig 5.6 b) Maximum Principal Stress

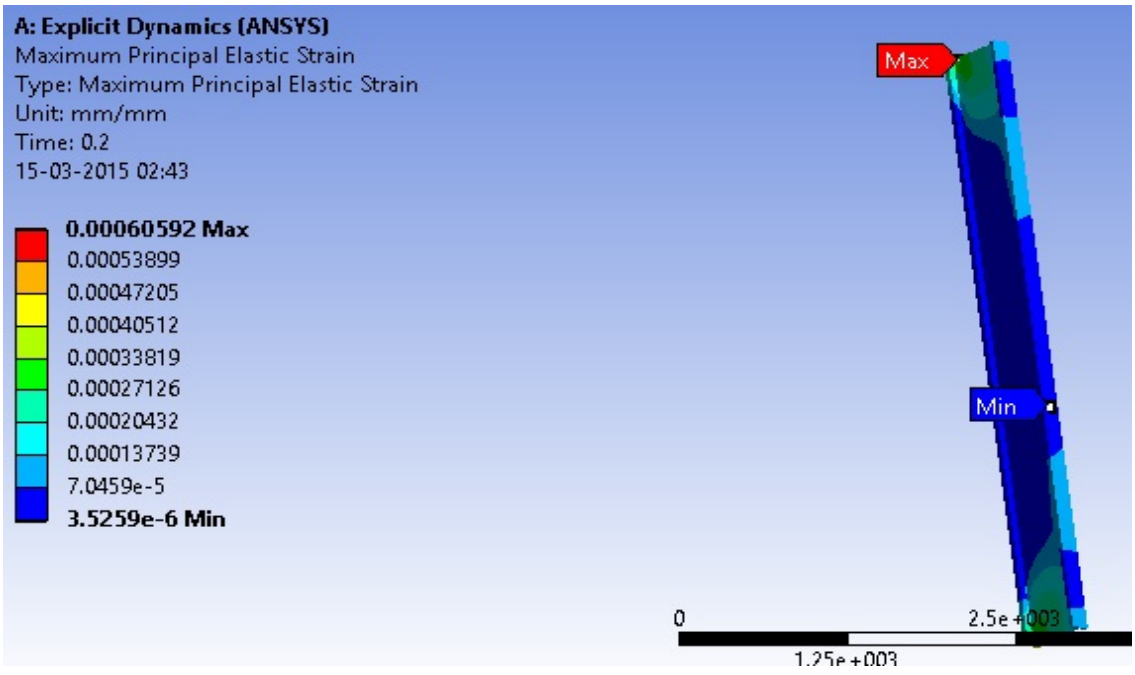

Fig 5.6 c) Maximum Principal Elastic Strain

Table 5.4 Response of Column Due to 100 kg TNT

STAND-OFF DISTANCE	**3m**	**4m**	**5m**
TOTAL DEFORMATION (mm)	4.1953	1.546	0.873
MAX. PRINCIPAL STRESS (Mpa)	352.3	98.43	52.43
MAX. PRINCIPAL ELASTIC STRAIN (mm/mm)	1.7e-03	5.20e-04	2.74e-04

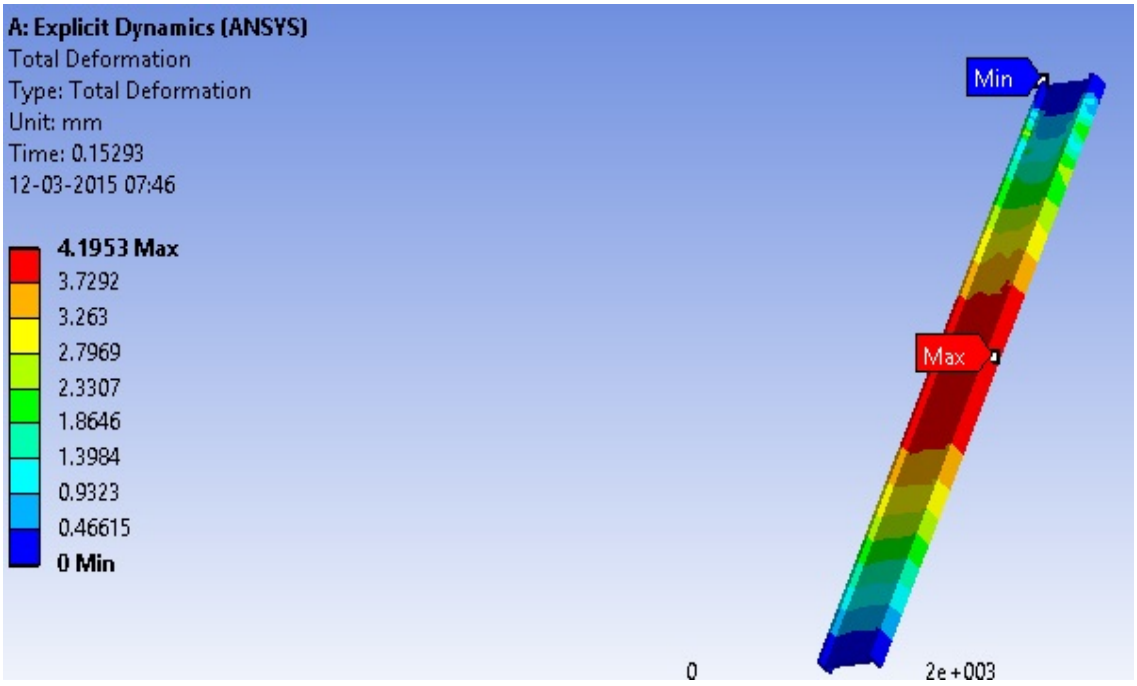

Fig 5.7 a) Maximum Deformation

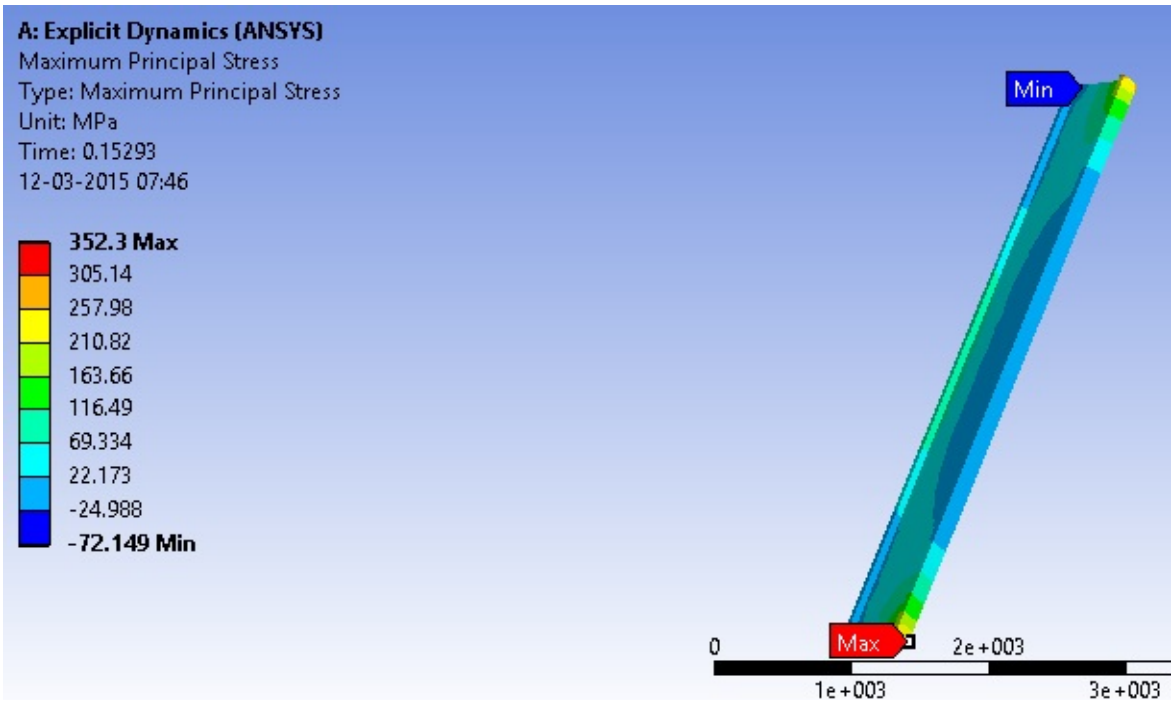

Fig 5.7 b) Maximum Principal Stress

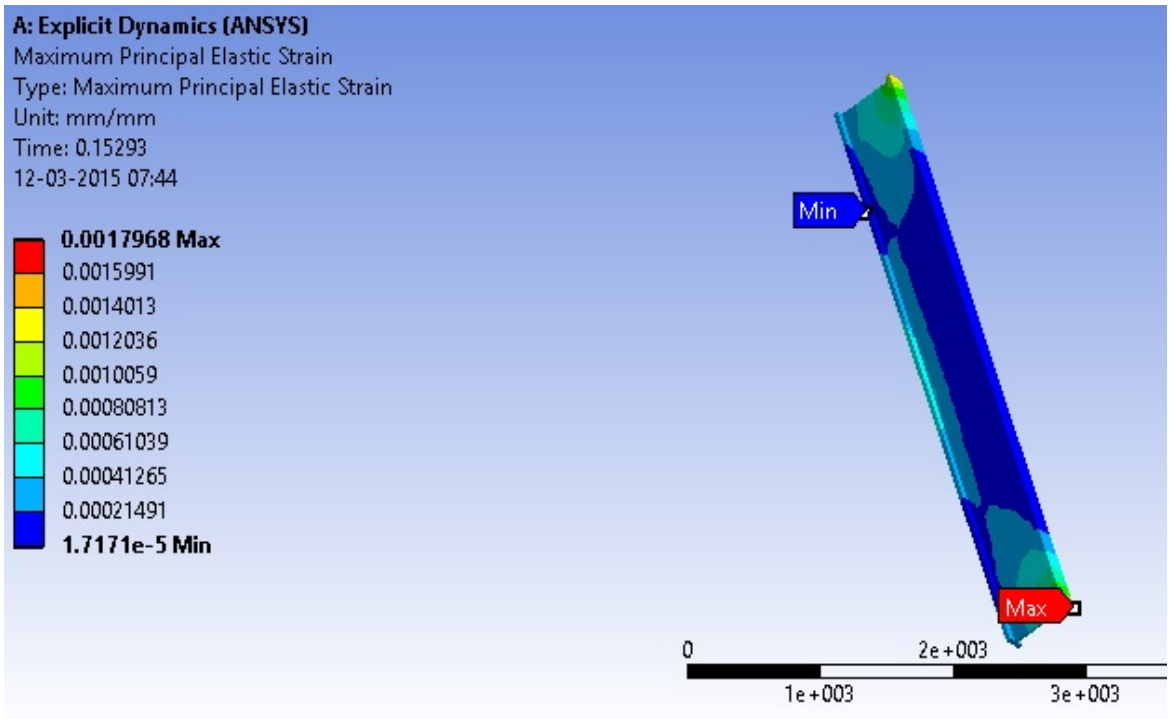

Fig 5.7 c) Maximum Principal Elastic Strain

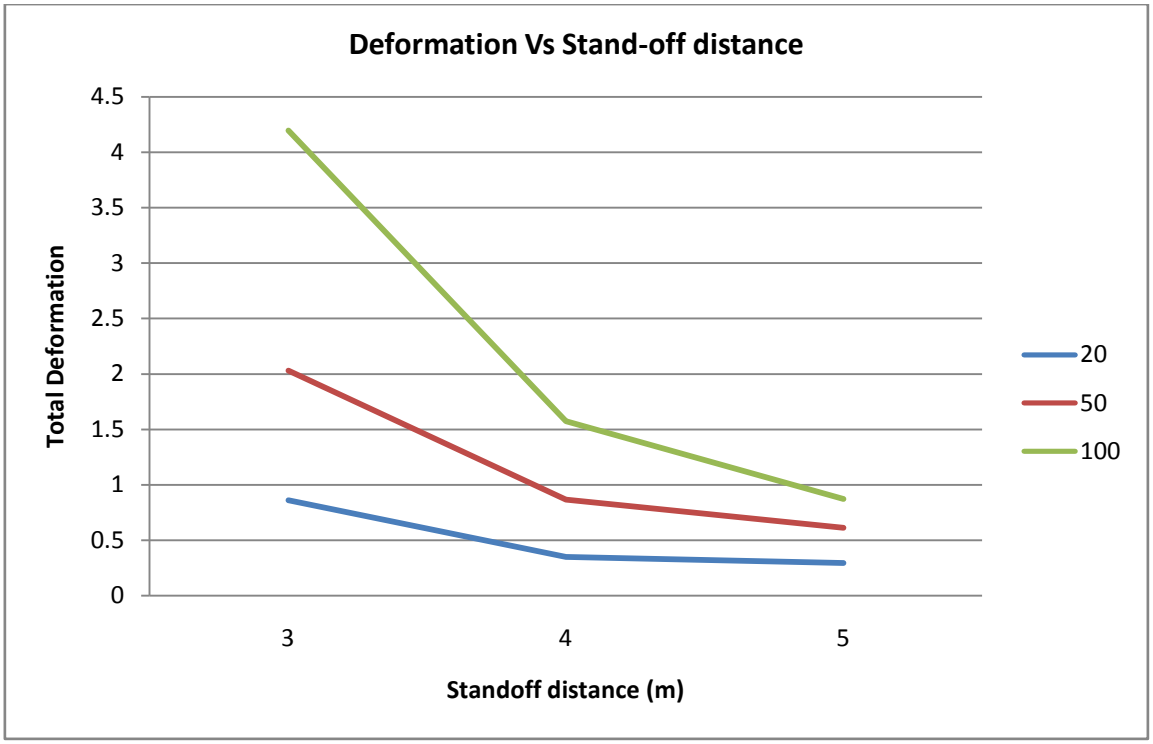

Fig 5.8 a) Deformation Vs Stand-off Distance Graph

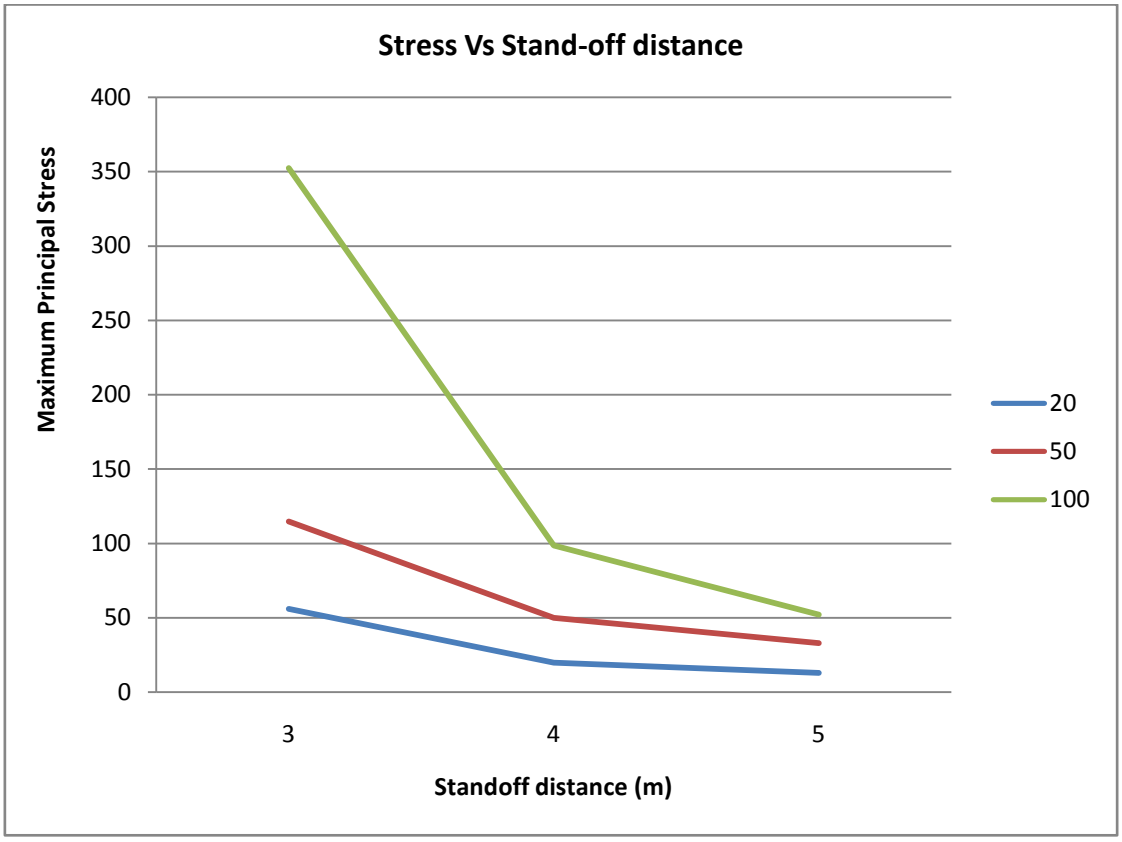

Fig 5.8 b) Stress Vs stand-off Distance Graph

The above graphs shows that at a specified distance and height higher charge weight effects more than a smaller charge weight in terms of total deflection and stress.

5.9 ANALYSIS IN ANSYS-AUTODYN

A steel column is taken from the above structure for the blast analysis which is much nearer to the explosive source i.e. at stand-off distance R = 1m with angel of incidence of 45 degree. The 1 kg of TNT produce 4184 kJ of energy based on that energy produced by 20 Kg , 50 Kg and 100 Kg was calculated and applied in analyses of steel column on ANSYS Autodyn-3D. The modelling of column is done in ANSYS Explicit Dynamic and properties of steel are as shown in Table 5.1 above.

The model is analysed in AUTODYN-3D and it is surrounded by air having ambient pressure of about 101.30 kPa. The analysis is done by using three material defined in ANSYS AUTODYN i.e. Steel, Air and TNT. Air is modelled as 2D Multi-fill material part.TNT filled using geometric shape and location of explosive is defined The AUTODYN environment and workspace with defined parts is as shown in Fig 5.9.

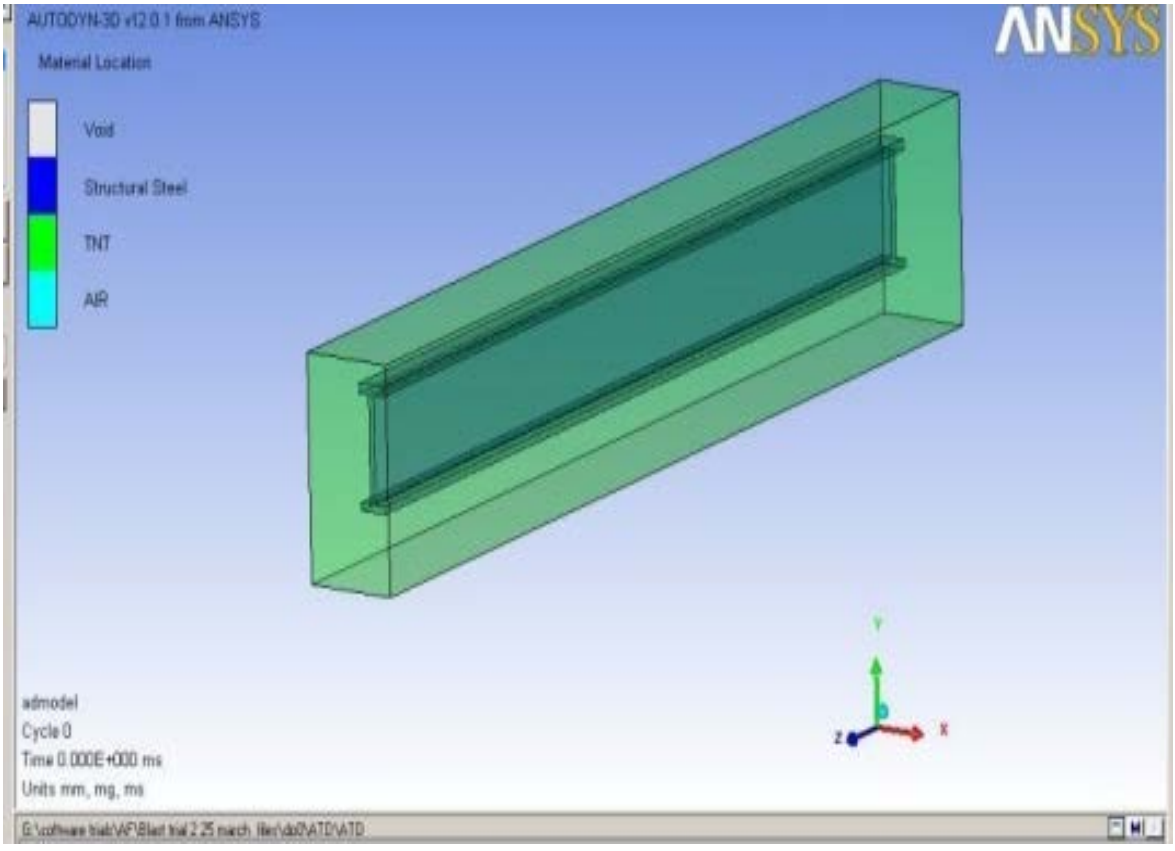

Fig 5.9 AUTODYN Environment

The density and internal energy of air and TNT which is used during the analysis is shown in Table 5.5

Table 5.5 Density and Internal Energy of Air and TNT

PARTS	DENSITY (g/cm3)	INT. ENERGY (J)
Air	0.00125	2.060e+005
TNT (1kg)	1.630	4.184e+006
TNT (20kg)	1.630	83.68e+006
TNT (50 kg)	1.630	209.2e+006
TNT(100 kg)	1.630	418.4e+006

5.10 RESULTS

The energy produced due to 20 kg TNT is about 83680 kJ causing total collapse of steel column after 1204 cycles at 0.426 ms (as shown in Fig 5.10). The pressure contour and Material summery are shown in Fig 5.11.

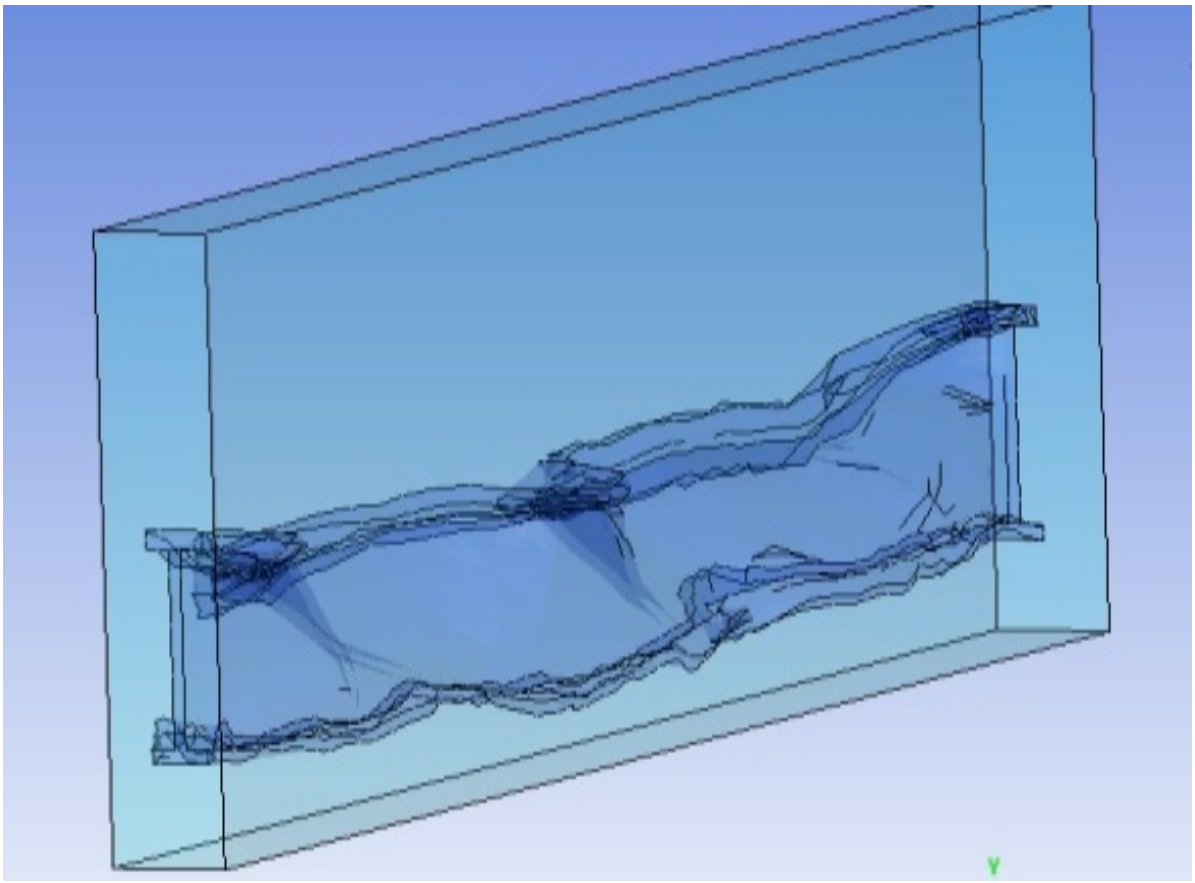

Fig 5.10 Total Collapse of Steel Due after 1204 cycle

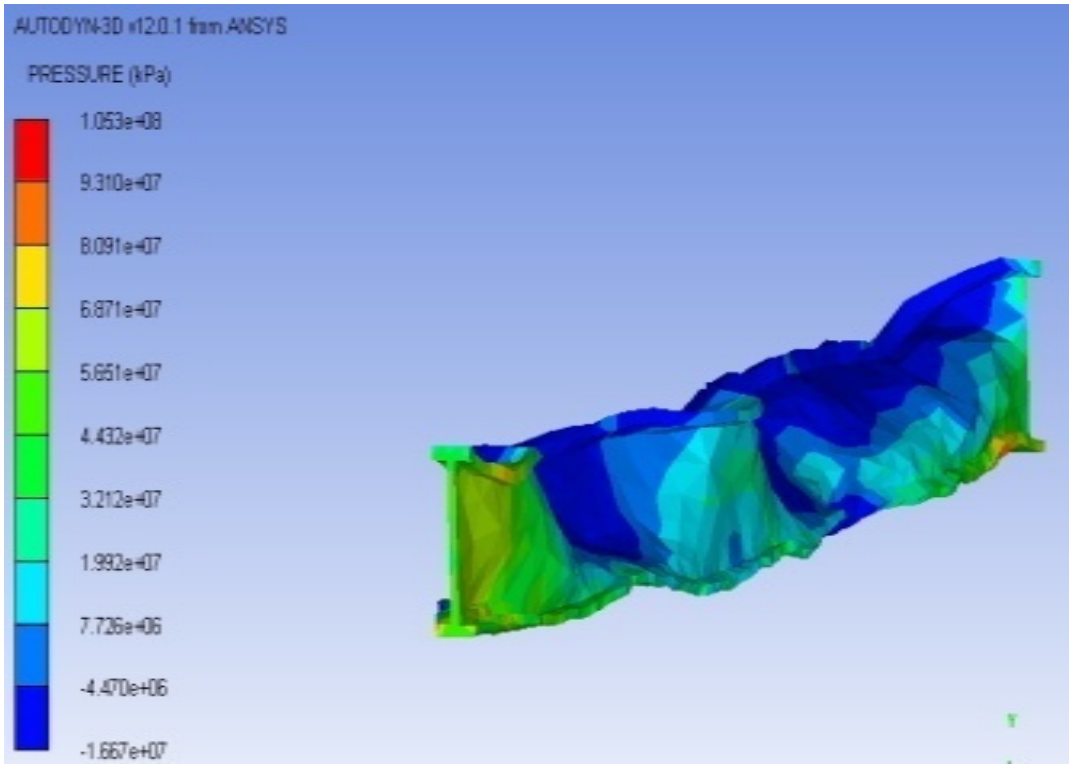

Fig 5.11 a) Pressure Contour

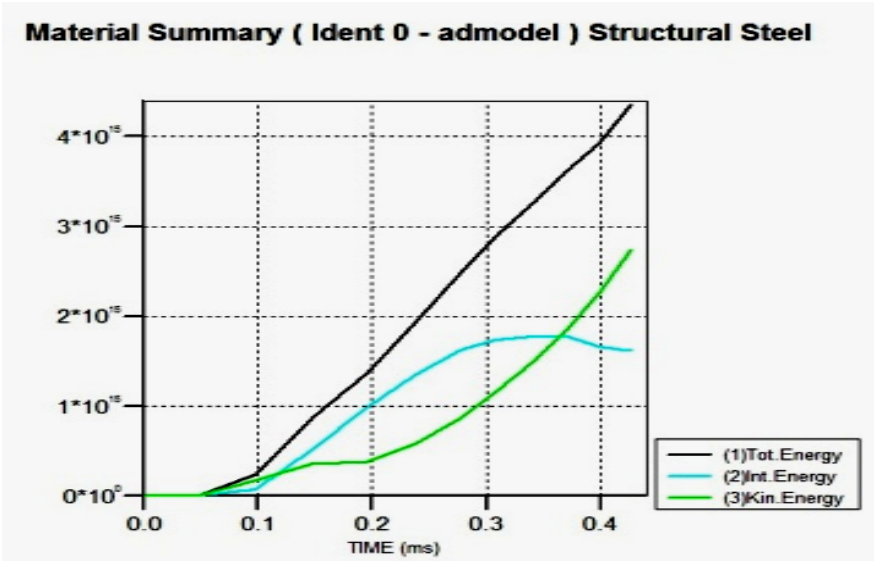

Fig. 5.11 b) Material Summery

TABLE 5.6:- MAX/MIN value of Energy

Minimum		Maximum	
X	Y	X	Y
0	1.000e-010	4.2639e-001	4.3467e+015
0	1.000e-010	3.1480e-001	1.7734e+015
0	1.000e-010	4.2639e-001	2.7265e+015

Similarly, the analysis of steel is done by applying energy produced due to 50 kg and 100 kg TNT as shown in Fig.

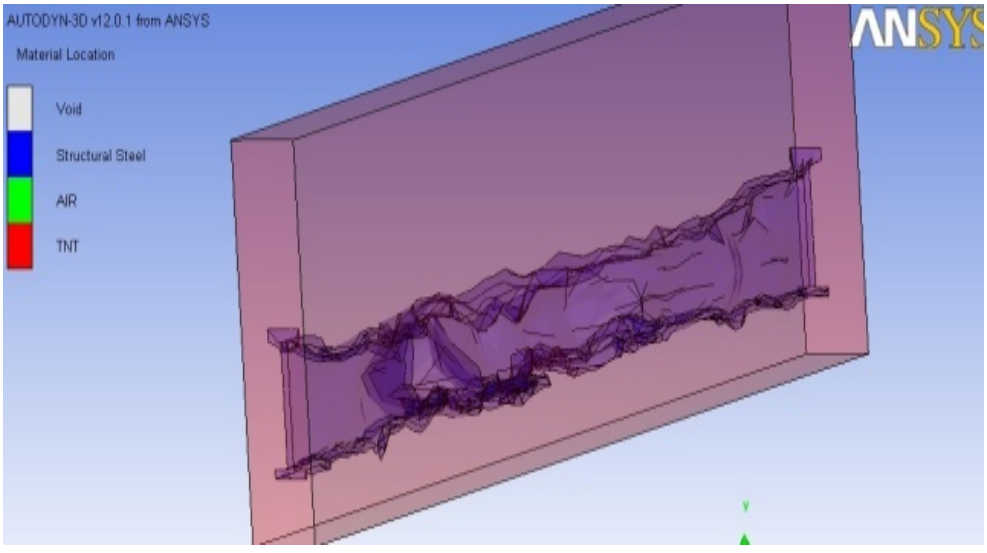

Fig 5.12 Total collapse after 950 cycles

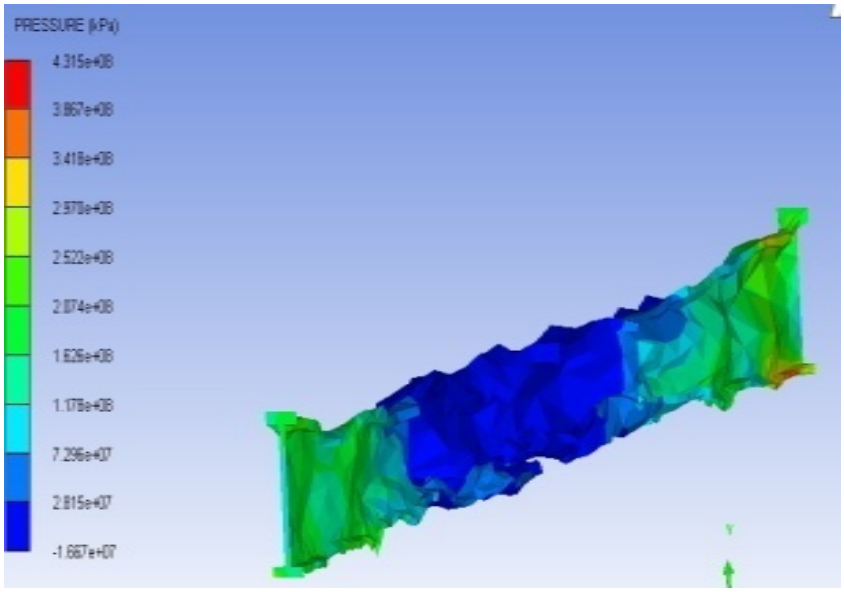

Fig 5.13 a) Pressure contour

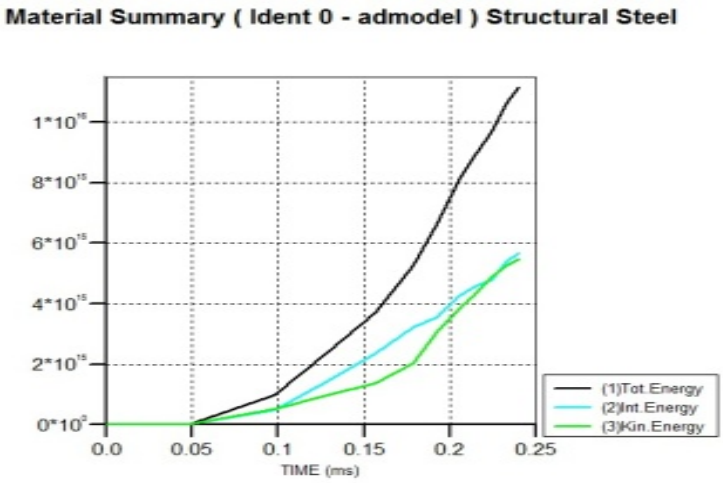

b) Material summery (50 kg)

Table 5.7: MAX/MIN value of Energy (50 kg)

Minimum		**Maximum**	
X	Y	X	Y
0	1.000e-010	2.4051e-001	1.1132e+016

0	1.000e-010	3.1480e-001	5.6654e+015
0	1.000e-010	2.4051e-001	5.4669e+015

Effect Due to 100 kg TNT

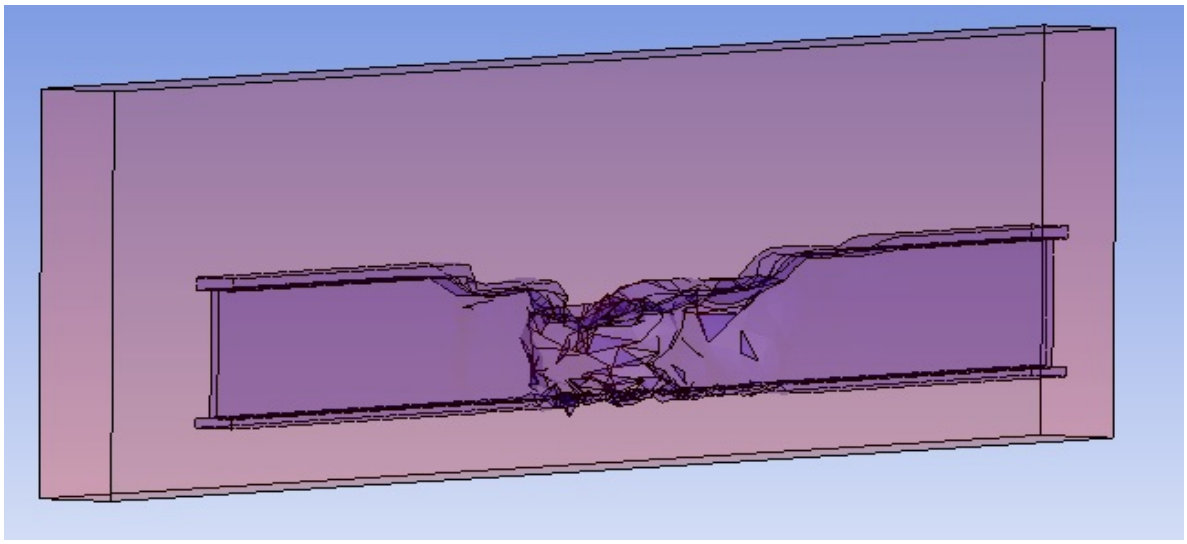

Fig 5.14 Total collapse after 587 cycles

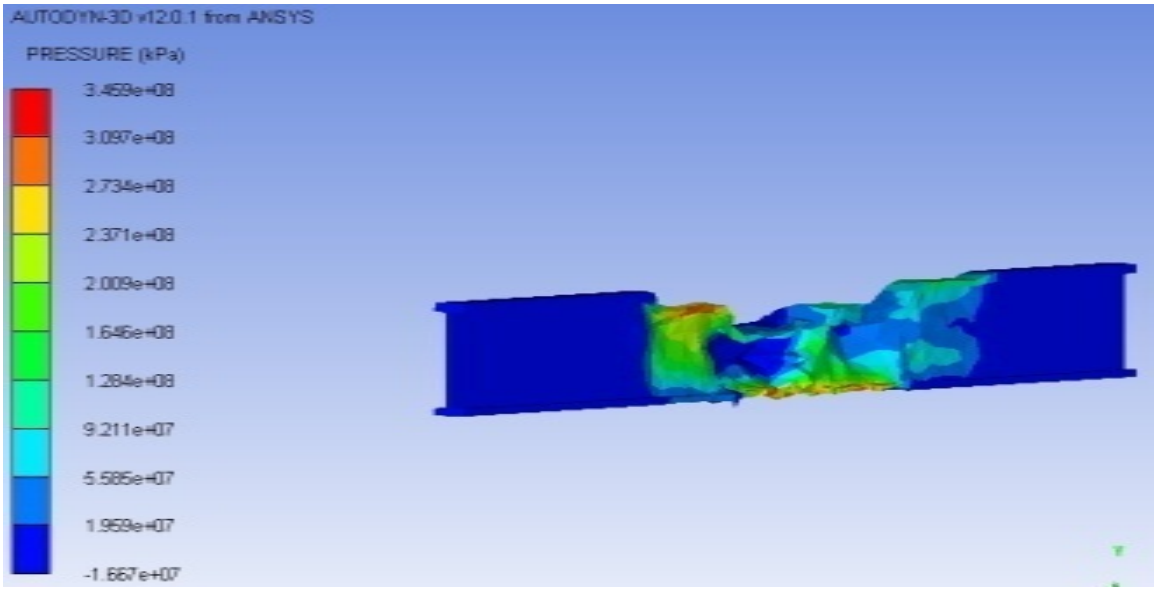

Fig 5.15 a) Pressure contour

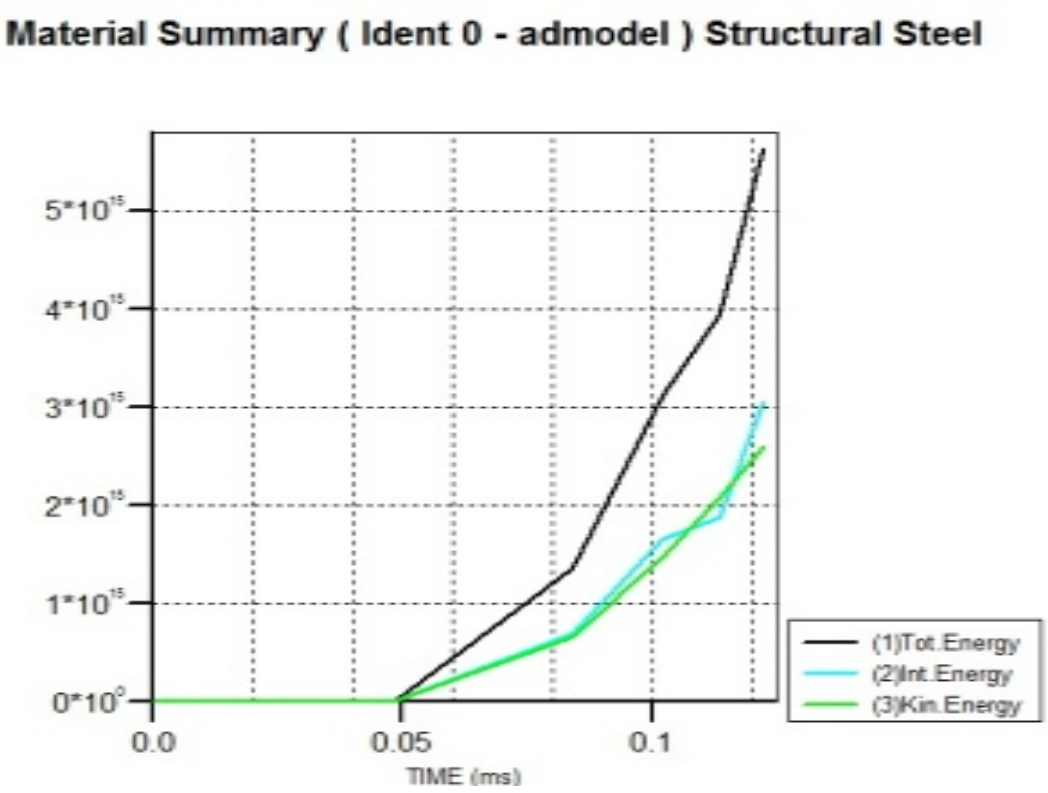

Fig. 5.15 b) Material summery (100 Kg)

TABLE 5.8 :- MAX/MIN value of Energy (100 kg)

Minimum		**Maximum**	
X	Y	X	Y
0	1.000e-010	1.2252e-001	5.6111e+015
0	1.000e-010	1.2252e-001	3.0369e+015
0	1.000e-010	1.2252e-001	2.5842e+015

The results obtained from the AUTODYN simulation analysis clearly signifies that how the energy produced during bomb explosion cause severe affect on mechanical properties of steel and will cause the total failure of steel within in few milliseconds. Results shows the progressive energy collapse of steel column under such a huge amount of energy which is released after the explosion.

5.11 BLAST EFFECTS ON CONCRETE WALL

In this section a M30 concrete wall with different shapes with and without steel plates is analyzed in ANSYS-Autodyn to study the behavior of concrete in such a high strain loading. The properties of concrete used is tabulated in Table 5.9

Table 5.9: Concrete Properties

Properties	Value	Units
Density	2400	kg/m^3
Young Modulus of Elasticity	30000	MPa
Poisson's Ratio	0.18	

CASE 1: Single Concrete Wall ((with and wihout Steel plate cladding)

The concrete wall is modelled in Explicit Dynamics module of ANSYS with the plan dimentions as 5m × 3m in X and Y directions, respectively with thickness of 0.2 m shown in Fig. 5.16a.

(B) Single Concrete Wall with Steel Plate Cladding

The same concrete wall with steel plate having thickness 0.005 m is shown in Fig 5.16b. The analysis is done by using a charge weight of 100 kg TNT at a heightof 1m above ground surface with a stand-off distance of 3m.

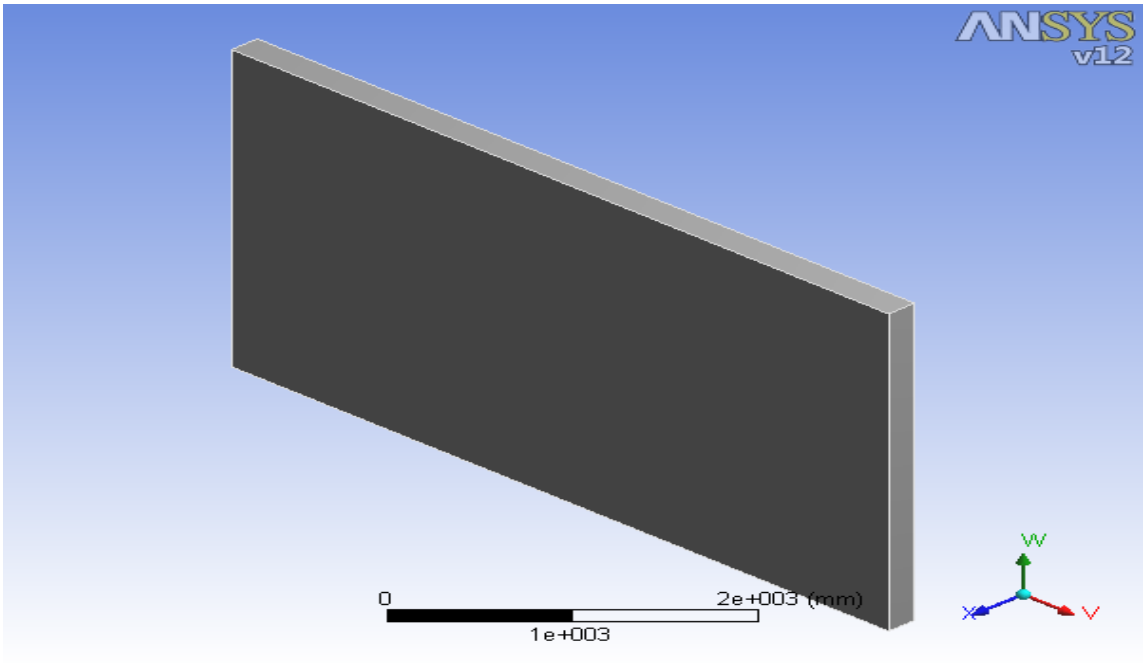

Fig 5.16 a) Geometry of Single Concrete wall without Steel plate

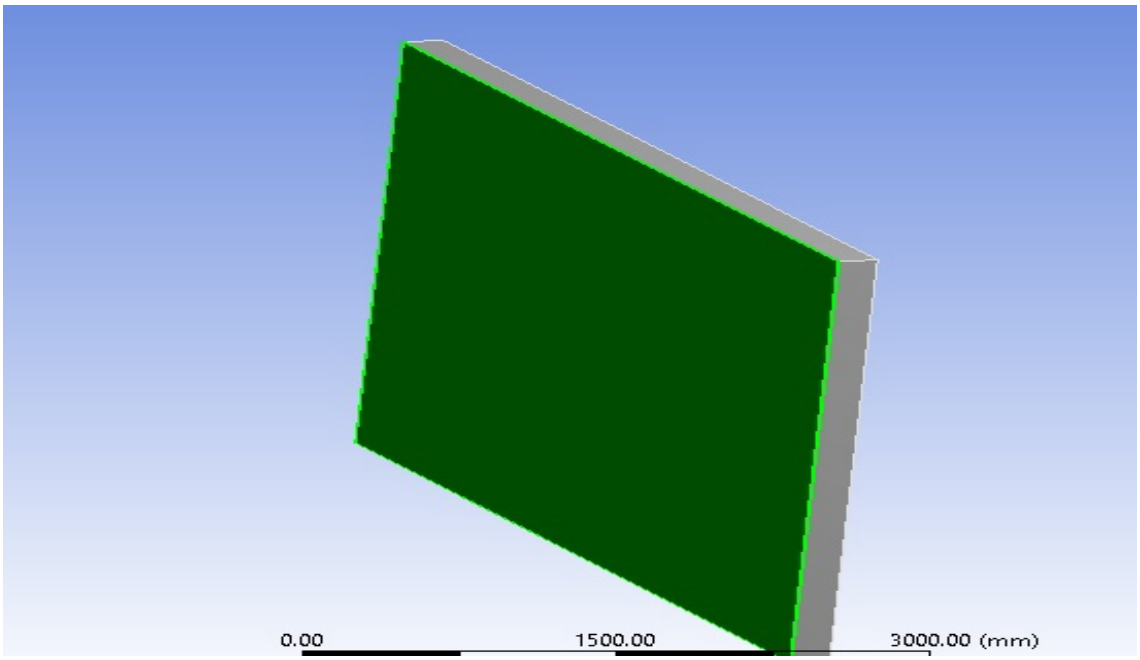

Fig. 5.16 b) Geometry of single concrete wall with steel plate

5.12 RESULTS

The concrete wall is firstly analysed for a pressure of 50 Mpa in FE Modeler and then transffered to Autodyn for blast scenerio. Analysis output is showed in terms of pressure contours and pressure time history in following section:-

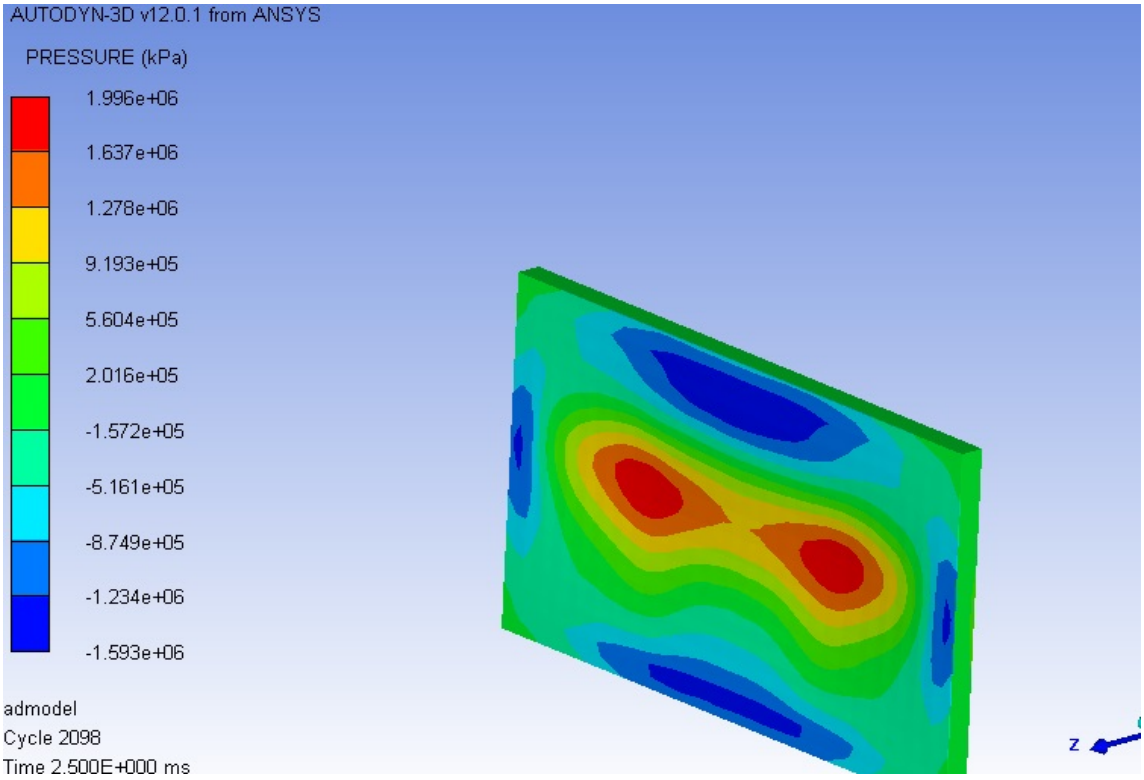

Fig 5.17 a) Pressure contour of wall without steel plate

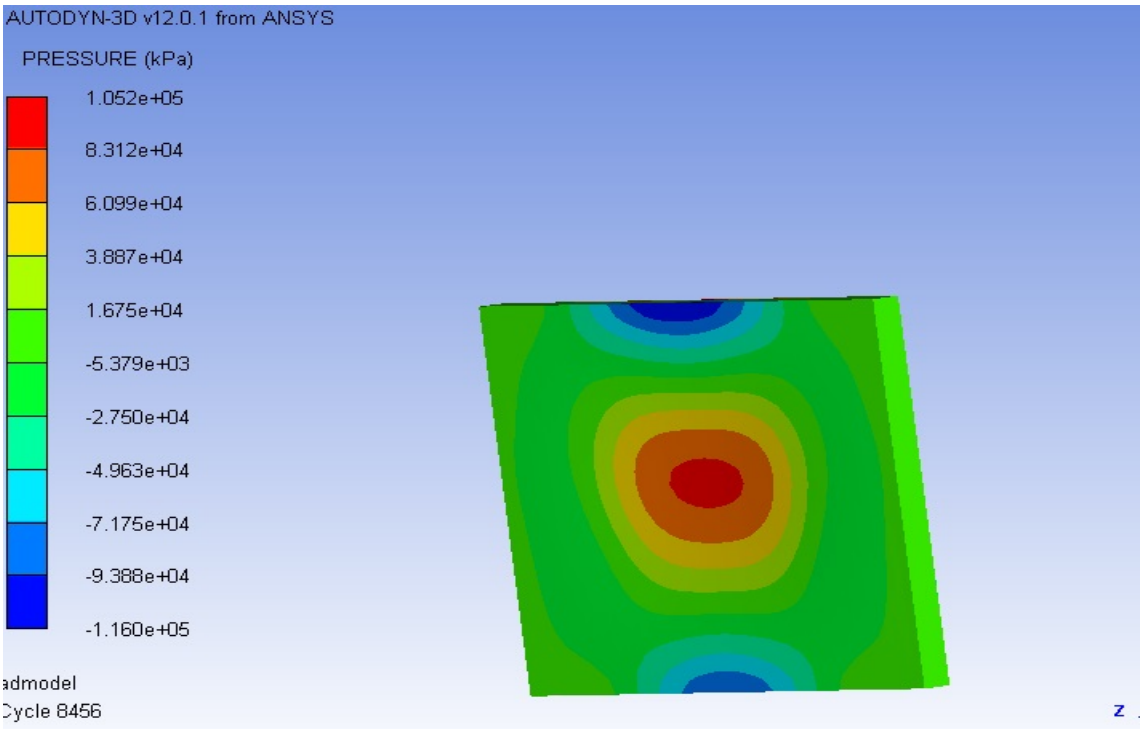

Fig 5.17 b) Pressure contour of wall with steel

Guage point is defined at the center of wall, thus pressure time history in both the cases is shown in Fig 5.18.

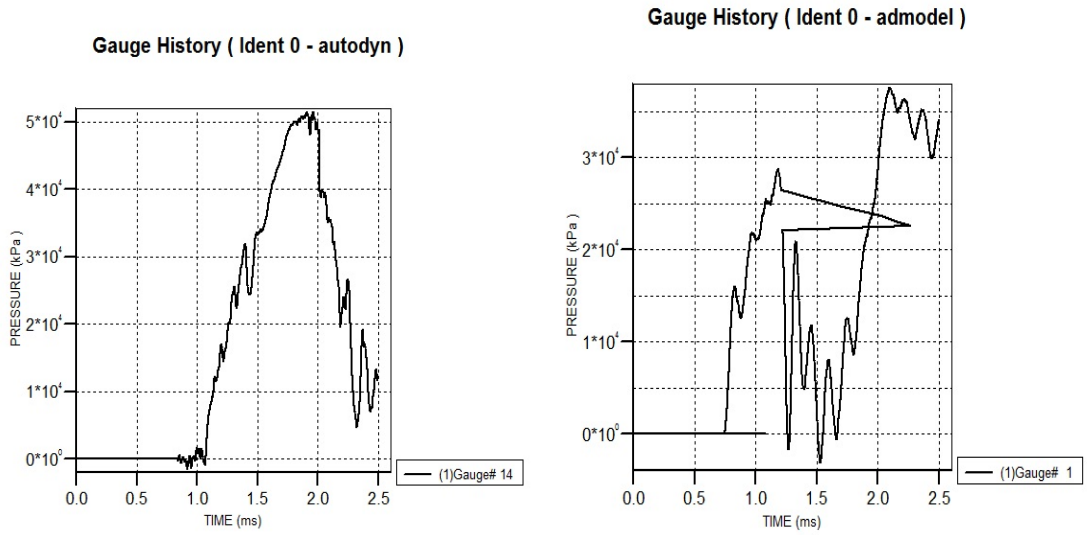

Fig 5.18 Pressure-time History plots

The pressure contour and time history plots clearly shows that by using a steel plate pressure on a concrete wall is reduced.

Case 2 :L-shape Concrete Wall ((with and wihout Steel plate cladding)

L-shape concrete wall is modelled in geometry module of Ansys Explicit Dynamic. Concrete wall without and with 5mm thick plate as shown in Fig. 5.19. Concrete wall is modelled as a solid part and guage points is defined at the centre of these 2 solid parts.Detonation point is define at a cordinate of -3000,1000,-3000 in X,Y and Z directions i.e. at an angel of 45 degree and at a height of 1m from joint. Pressure contour and time history plot at defined gauge point is shown in Fig 5.20 and Fig 5.21.

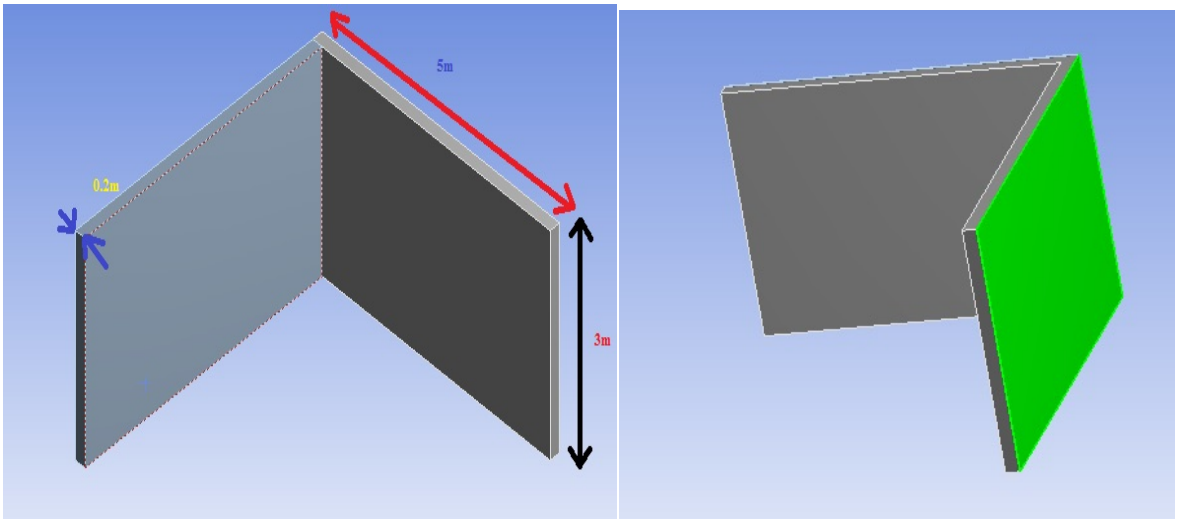

Fig 5.19 Geometry of L-shape concrete wall without steel plate and with steel plate

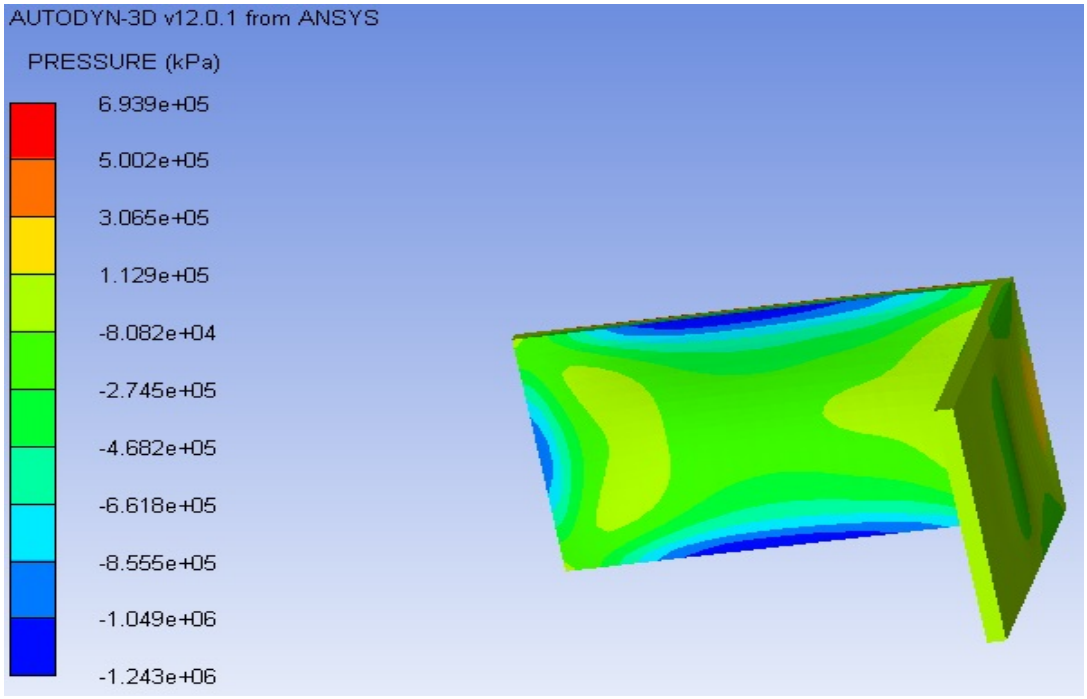

5.20 a) Pressure contour without steel plate

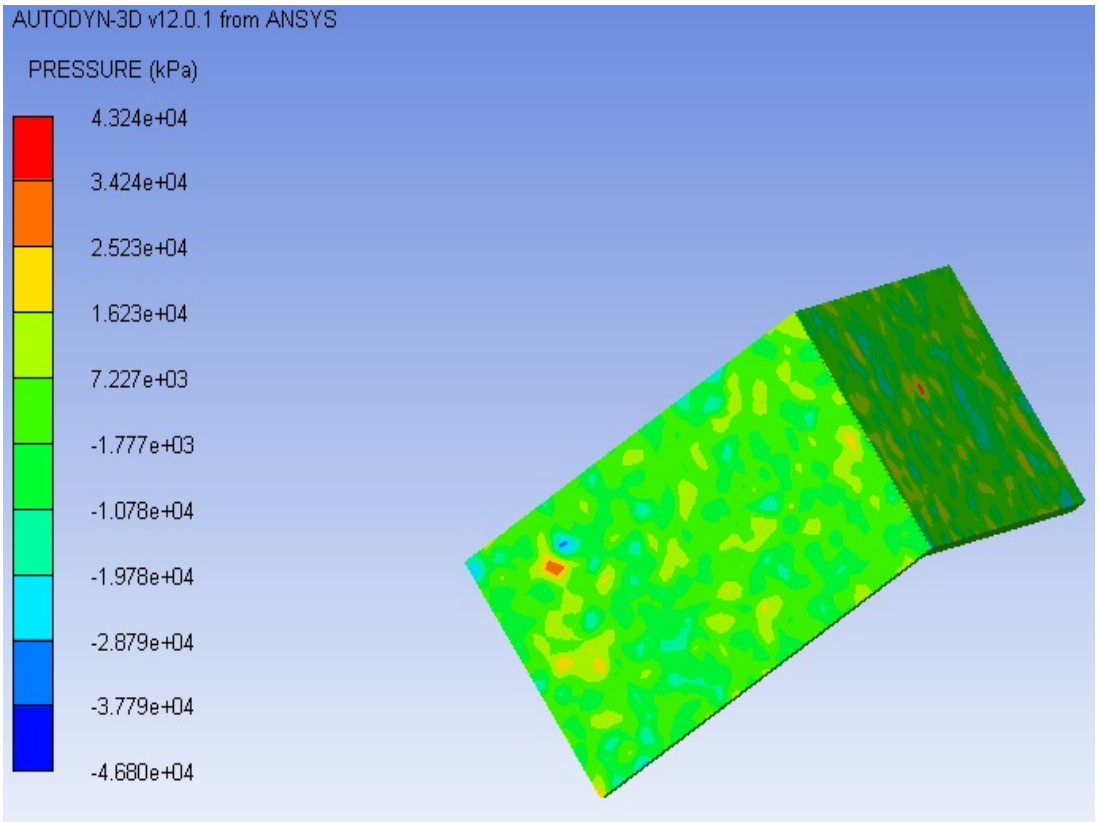

Fig 5.20 b) Pressure contour with steel plate

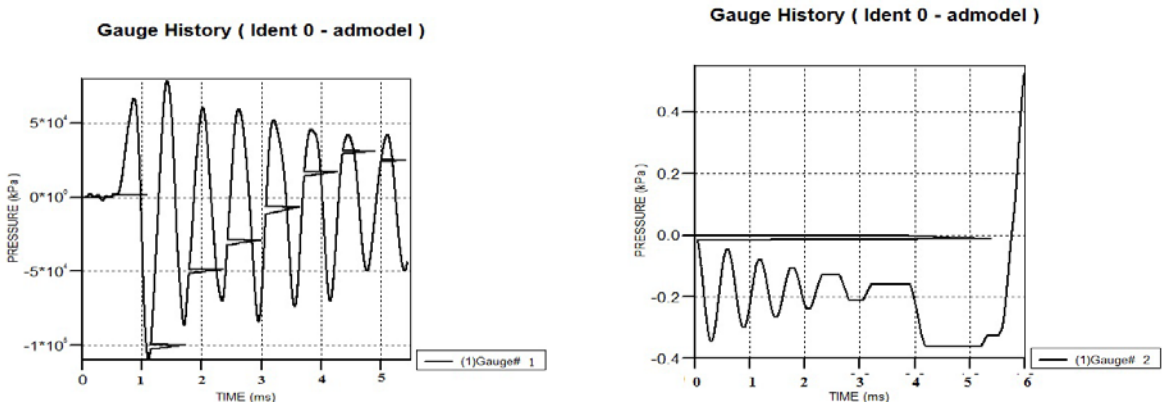

Fig 5.21 Pressure Time history without and with steel plate

The pressure time history plots shows that in case of L- shape wall without steel plate blast pressure flactuates throughout the cycle but in case wall with steel plate pressure is initially negetive but after complition of certain cycle the value changes to positive itsel. This is due to the bonded steel plate. Also it is found that pressure is reduced by large amount due to steel plate.

Case 3: C-Shape wall (with and wihout Steel plate cladding)

Another shape of concrete wall is used to study the behaviour of blast pressure on wall without steel plate and with steel plate. The geometry of C-shape (in plan) concrete wall along with dimensions is as shown in Fig 5.22.

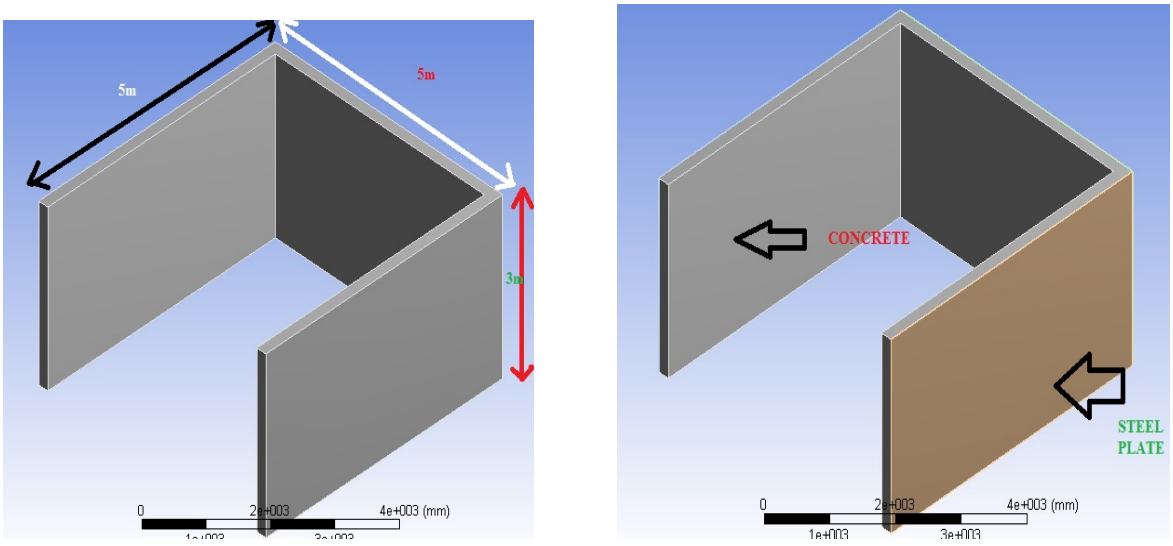

Fig 5.22 Geometry of U shape wall without and with steel plate

The detonation point is same as used in case 2 and gauge point are defined at the centre of middle wall. End conditions are fixed and steel plate is bonded with concrete at the outer side which is in front of explosion source. The pressure contour without and with steel plate is shown in fig 5.23a and 5.24b.

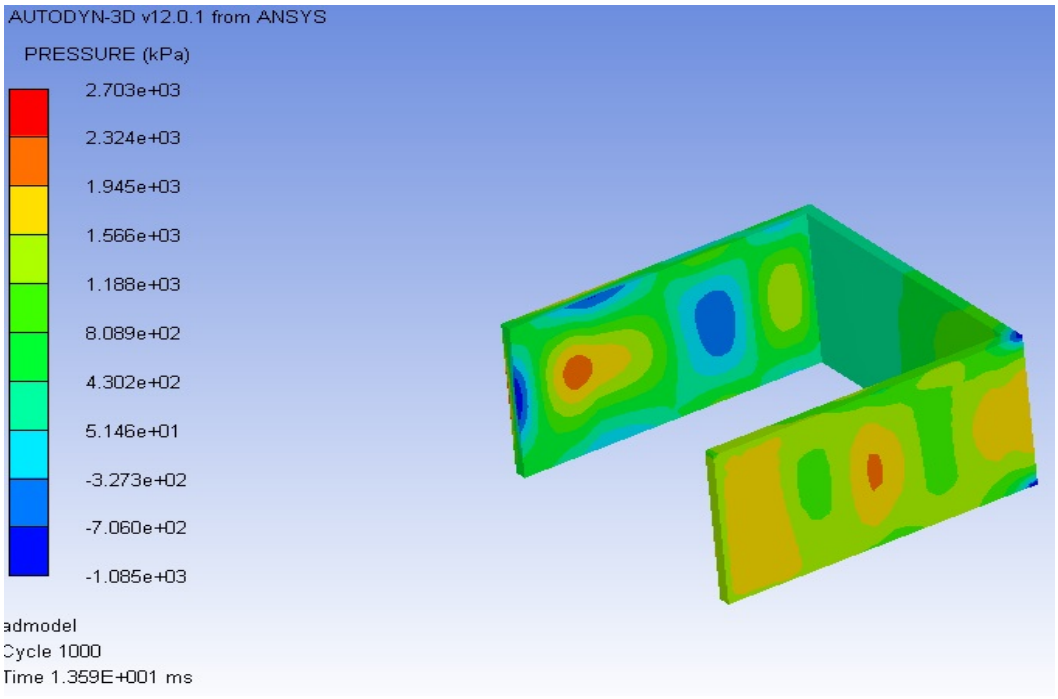

Fig 5.23 a) Pressure contour of wall without steel plate

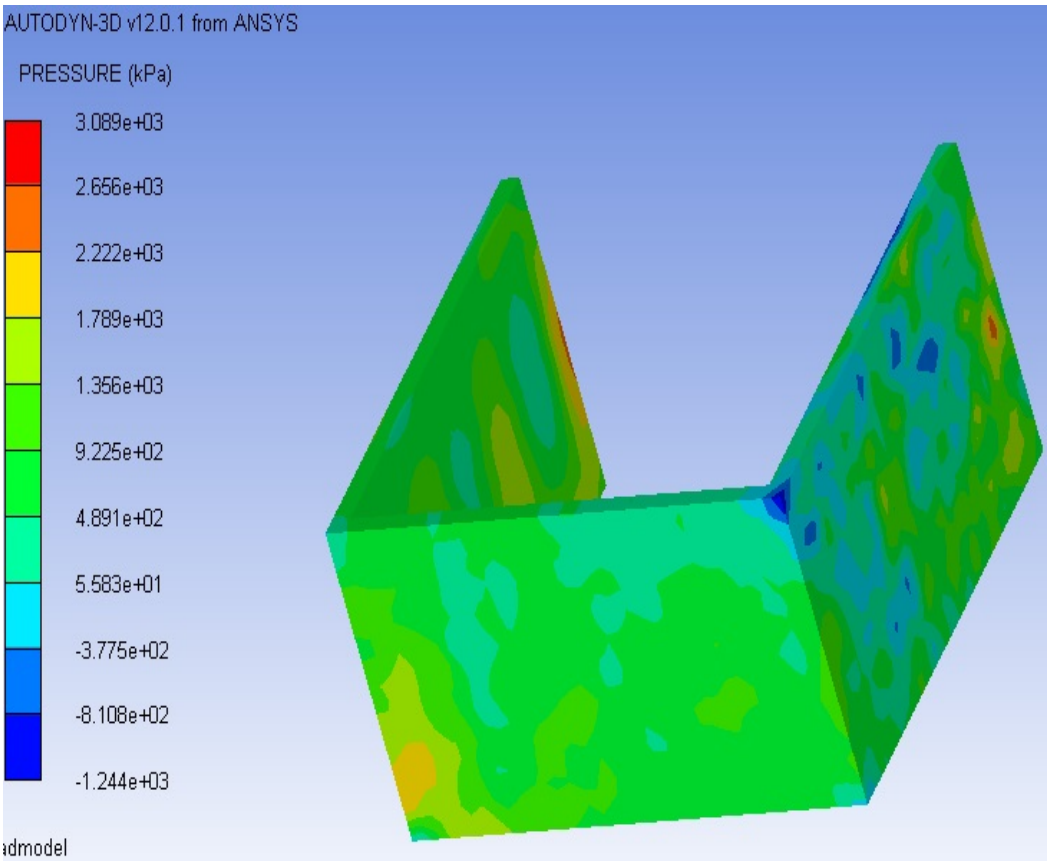

Fig 5.23 b) Pressure contour after using steel plate

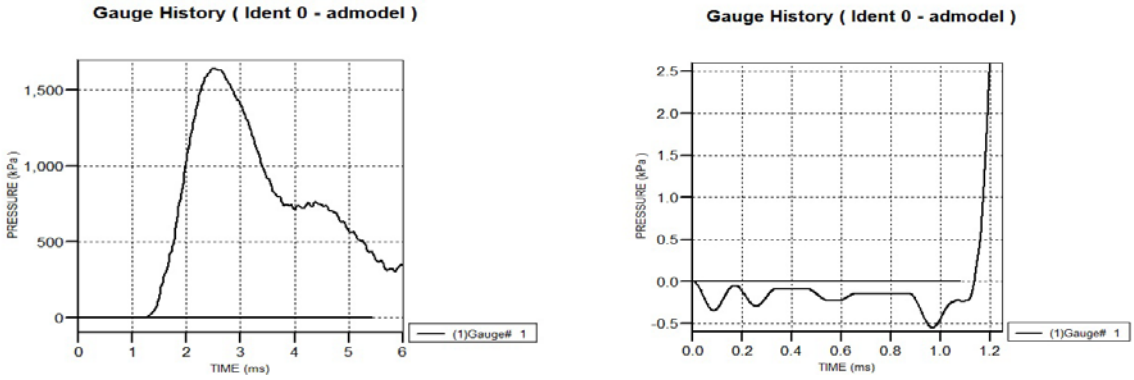

Fig 5.24 Pressure Time history plots

Pressure time history plots clearly shows the the impact and pressure on concrete wall is reduced by large amount by using a 5mm thick plate. It has been observed that in case of steel plate with concrete wall intially pressure is nagative but after some cycles and time the pressure becomes positive but less then pressure on concrete wall without steel plate.

CHAPTER 6
CONCLUSIONS

6.1 CONCLUSIONS

It is observed from literature survey that for the estimation of blast load or pressure the empirical approach (Kinney and Graham's) proves to be ideal as blast phenomenon is complex in nature. Complexity arises due to unpredictability of charge weight and standoff distance, the behaviour of material under different loading conditions and post blast trigerring events. Ansys Autodyn is an efficient and user friendly tool for simulating eplosives and impact loading linking it with workbench envirnoment. The blast simulation was carriout using JWL as equation of state for explosive materials. The two storey steel structure was subject to singel charge weights and standoff distances to obtain output parameters like, deflection and joint reactions using SAP2000. A steel column from the above structure is subjected to different charge weight and standoff distance to obtain the parameter like total deformation, maximum principal stress and maximum principal starin and the same column is analysed in Aotudyn to obtain the progressive energy collapse of steel. The concrete walls of different shapes shapes with or without steel plates cladded are analysed in Autodyn to obtain pressure contours and pressure time history plots to study the behaviour and effect of using steel. From the present study the following observations and conclusions are drawn .

1. Blast load on structure cause formation of high reactions on joints leads to shear collapse of joints and total collapse of structure.
2. Analysis of steel column in ANSYS Explicit dynamics clearly specifies that effect of explosion largely depends upon the standoff distance and charge weight.
3. Large deformation is obtained at higher charge weight for a given same standoff distance as evident from graph.
4. Higher stresses have been observed with higher charge weight then with the lower charge weights as evident from table and graph.
5. The finite element analysis revealed that, for axially loaded columns, there exists a critical lateral blast impulse. Any applied blast impulse above this value will result in the collapsing of the column before the allowable beam deflection criterion is reached.

6. For higher charge weights, the collapse occurs faster, as is evident from the graphs. The column fails in half the time for 50 kg TNT than for 20 kg TNT, whereas for 100 kg TNT, it takes about one-fourth the time to fail than 20 kg TNT.
7. In case of 20 kg TNT blast, the internal energy of the steel column reduces after about 0.35 ms of loading, while no reduction in this energy is seen for charge weights beyond this value. This occurs prior to failure starts.
8. For 20 kg and 50 kg charge weights, the internal energy remains beyond kinetic energy until failure starts, while for 100 kg charge weights, both the energies remain approximately the same. This may be attributed to the very high impulse pressure of shock waves for higher TNT weights.
9. Autodyn Simulation gave good estimate of pressure time history of observed positive and negative phase.
10. Pressure contour and time history plots signify that using a steel plate reduces the effect of blast pressure on the concrete wall thus reducing the damage due to pressure created by the 100 kg TNT with standoff distance and height of 3 m and 1 m. Similar observation goes for other plan shapes.
11. The column response to non-uniform blast loads was shown to be significantly influenced by higher vibration modes. This was especially true for the unsymmetrical blast loads.
12. For high-risks facilities such as public and commercial tall buildings, design considerations against extreme events (bomb blast, high velocity impact) are require.

SCOPE OF FURTHUR WORK

The following may be considered for the possible extension to the work presented herein.

1. Verification of pressure computation done by Kinney Graham's approach by JWL approach using any FEM program such as ABAQUS, Autodyn or LS-Dyna.
2. Exploring the possibility of disproportionate collapse of steel building considered due to column failure.
3. In depth failure analysis of column and walls facing blast considering high-strain rate loading.

REFERENCES

1. A. Khadid et al. (2007), " Blast loaded stiffened plates" Journal of Engineering and Applied Sciences,Vol. 2(2) pp. 456-461.
2. A.K. Pandey et al. (2006) "Non-linear response of reinforced concrete containment structure under blast loading" Nuclear Engineering and design 236. pp.993-1002.
3. Alexander M. Remennikov, (2003) "A review of methods for predicting bomb blast effects on buildings", Journal of battlefield technology, vol 6, no 3. pp 155-161.
4. American Society for Civil Engineers 7-02 (1997), "Combination of Loads",pp 239-244.
5. ANSYS Theory manual, version 5.6, 2000.
6. Biggs, J.M. (1964), "Introduction to Structural Dynamics", McGraw-Hill, New York.
7. D.L. Grote et al. (2001), "Dynamic behavior of concrete at high strain rates and pressures", Journal of Impact Engineering, Vol. 25, Pergamon Press, NewYork, pp. 869-886, 10. IS 456:2000 Indian Standard Plain and Reinforced Concrete Code of Practice.
8. J.M. Dewey (1971), "The Properties of Blast Waves Obtained from an analysisof the particle trajectories", Proc. R. Soc. Lond. A.314, pp. 275-299.
9. J.M. Gere and S.P. Timoshenko (1997.), "Mechanics of materials", PWS publishing company, Buston, Massachusetts, 66.
10. Kirk A. Marchand, Farid Alfawakhiri (2005), "Blast and Progressive Collapse" fact for Steel Buildings, USA.
11. M. V. Dharaneepathy et al. (1995),"Critical distance for blast resistance design", computer and structure Vol. 54, No.4.pp.587-595.
12. Nelson Lam et al. (2004), "Response Spectrum Solutions for Blast Loading", Journal of Structural Engineering, pp 28-44.
13. P. Desayi and S. Krishnan (1964), "Equation for the stress-strain curve of concrete". Journal of the American Concrete Institute, 61, pp 345-350.
14. S.Unnikrishna Pillai and Devdas Menon(2003), "Reinforced Concrete Design", Tata McGraw-Hill.
15. Ronald L. Shope (2006), "Response of wide flange steel columns subjected to constant axial load and lateral blast load". Civil Engineering Department, Blacksburg, Virginia

16. Schmidt, Jon A. (2003), “Structural Design for External Terrorist Bomb Attacks”, STRUCTURER magazine, March issue.
17. S.Unnikrishna Pillai and Devdas Menon (2003) , “Reinforced Concrete Design”, Tata McGraw-Hill, pp 121-196.
18. T. A. Rose et al. (2006), “The interaction of oblique blast waves with buildings”, Published online: 23 August 06 © Springer-Verlag, pp 35-44.
19. T. Borvik et al.(2009) “Response of structures to planar blast loads – A finite element engineering approach” Computers and Structures 87, pp 507–520.
20. TM 5-1300(UFC 3-340-02) U.S. Army Corps of Engineers (1990), “Structures to Resist the Effects of Accidental Explosions”, U.S. Army Corps of Engineers, Washington, D.C., (also Navy NAVFAC P200-397 or Air Force AFR 88-2.